Materials Horizons

Biofabrication of vascularized adipose tissues and their biomedical applications

Journal:	*Materials Horizons*
Manuscript ID	MH-REV-11-2022-001391.R1
Article Type:	Review Article
Date Submitted by the Author:	18-Jan-2023
Complete List of Authors:	Karanfil, Aslı; Osaka University, Department of Applied Chemistry Louis, Fiona; Osaka University, Joint Research Laboratory (TOPPAN) for Advanced Cell Regulatory Chemistry, Graduate School of Engineering Matsusaki, Michiya; Osaka University, Graduate School of Engineering, Department of Applied Chemistry

SCHOLARONE™
Manuscripts

Please do not adjust margins

ARTICLE

Biofabrication of vascularized adipose tissues and their biomedical applications

Received 00th January 20xx,
Accepted 00th January 20xx

DOI: 10.1039/x0xx00000x

Aslı Sena Karanfil,[a] Fiona Louis [b] and Michiya Matsusaki*[a,b]

Recent advances in adipose tissue engineering and cell biology have led to the development of innovative therapeutic strategies in regenerative medicine for adipose tissue reconstruction. To date, the many *in vitro* and *in vivo* models developed for vascularized adipose tissue engineering cover a wide range of research areas, including studies with cells of various origins and types, polymeric scaffolds of natural and synthetic derivation, models presented using decellularized tissues, and scaffold-free approaches. In this review, studies on adipose tissue types with different functions, characteristics and body locations have been summarized with 3D *in vitro* fabrication approaches. The reason for the particular focus on vascularized adipose tissue models is that current liposuction and fat transplantation methods are unsuitable for adipose tissue reconstruction as the lack of blood vessels results in inadequate nutrient and oxygen delivery, leading to necrosis *in situ*. In the first part of this paper, current studies and applications of white and brown adipose tissues are presented according to the polymeric materials used, focusing on the studies which could show vasculature *in vitro* and after *in vivo* implantation, and then the research on adipose tissue fabrication and applications are explained.

1. Introduction

Adipose tissue (AT) is a unique tissue representing 10-30% of the total body weight, and plays a role in regulating body homeostasis with important endocrine and secretion functions [1–3]. Main cells in AT cells are called adipocytes and act as energy stores due to the high lipid content in their cytoplasm [4]. Apart from adipocytes, AT has a dynamic cellular content called stromal vascular cells (SVC) including fibroblasts, smooth muscle cells, pericytes, endothelial cells and preadipocytes [2,5]. Because of these rich cellular ingredients, AT has an important function for whole body metabolism [2].

There are basically two types of AT: white and brown [6,7]. However, other AT types and characteristics including beige/bright, pink and yellow have also been described in the literature [1,8,9] (Fig. 1). While white adipose tissue (WAT) consists of adipocytes containing a single and large lipid vesicle which serves as an energy store in the body, brown adipose tissue (BAT) includes adipocytes with a large number of small lipid droplets and its main function is thermoregulation [10,11]. A good balance of these two AT types is needed to maintain energy homeostasis in the body [7,12].

The global rise in obesity and related metabolic comorbidities has led to an increase in the importance of studies on ATs.

Developments in regenerative medicine and tissue engineering, in particular, allow three-dimensional (3D) fabrication of living tissues *in vitro* and diversification of approaches to soft tissue engineering [12–14]. In addition to *in vitro* research and applications, the production of 3D AT models that allow *in vivo* transplantation is within the scope of soft tissue engineering studies in terms of cosmetic, reconstructive or therapeutic approaches [1]. On the other hand, autologous fat graft transplantations have played a vital role in clinical studies performed to date, but they have significant disadvantages such as donor side morbidity and lack of graft persistence [15,16]. Studies to date show that vascularized AT models are in demand to elucidate the mechanisms of common diseases, to screen for new drugs, or to assess drug safety levels [17,18]. However, the main challenge limiting clinical applications of engineered tissues for soft tissue production is vascularization [18,19]. Therefore, vascularization of grafts is a basic requirement for the production of large-scale functional ATs [20]. In addition, fat graft resection or necrosis encountered after transplantation is the result of inadequate vascularization, which leads to inadequate nutrient and oxygen delivery [14]. These problems must be overcome to obtain a viable product. Appropriate vasculature might also be essential to mimic organ-level functions for *in vitro* models and is thus a requirement to recapitulate organ-scale drug screening [21].

AT engineering is a growing and challenging area of research, covering current clinical needs for a variety of AT pathologies and defects [8,15]. On one hand, in research on WAT engineering, soft tissue production for plastic and reconstructive surgery is the basic aim [14,22]. BAT engineering, on the other hand, is a relatively new field of research that is carried out to recapitulate complex thermogenic cell functions for *in vitro* scenarios [23,24].

[a] *Department of Applied Chemistry, Graduate School of Engineering, Osaka University, Japan. E-mail: m-matsus@chem.eng.osaka-u.ac.jp*
[b] *Joint Research Laboratory (TOPPAN) for Advanced Cell Regulatory Chemistry, Graduate School of Engineering, Osaka University, Japan.*
† Footnotes relating to the title and/or authors should appear here.
Electronic Supplementary Information (ESI) available: [details of any supplementary information available should be included here]. See DOI: 10.1039/x0xx00000x

Please do not adjust margins

1.1. Types of adipose tissues

1.1.1. White adipose tissue

Characterized by adipocytes containing large unilocular lipid droplets, WAT is an active endocrine organ which plays an active role in the regulation of physiological and metabolic processes in the body [25], regulating various activities such as insulin sensitivity, lipid metabolism and satiety [5]. It constitutes 9-18% and 14-28% of body weight in lean men and women, respectively [26] and is generally located in the subcutaneous regions of the body, around the internal organs and in the facial area [5]. It is also found as large deposits in the abdomen (omentum), in the intestine (mesentery) and perirenal areas (retroperitoneum) and subcutaneously in the hips, thighs and abdomen [7].

Adipocytes, the main cellular component of WAT, are lipid-filled cells supported by collagen fibers, constituting approximately 90% of the cytoplasm of a mature white adipocyte [4] (Fig. 1c). Mature adipocytes in the WAT are found in large (up to 290 µm cell diameter), spherical form, surrounded by smaller preadipocytes, nerves and capillaries filling the interstitial spaces, and are arranged in a honeycomb-like geometry [27]. Each adipocyte is in contact with the vascular network which allows the tissue to grow continuously [28]. Besides adipocytes, various cell types are found in the tissue, such as preadipocytes, macrophages, neutrophils, lymphocytes and endothelial cells (ECs). The relationship and balance between these different cell types is closely related to the maintenance of full tissue homeostasis [29].

1.1.2. Brown adipose tissue

Brown adipose tissue (BAT) has been identified as the key thermogenic tissue in mammals [30]. Brown adipocytes, the main component of BAT, are morphologically different from white adipocytes due to their features such as a higher mitochondrial content and extracellular matrix (ECM) ratio, a large number of small lipid vesicles and an apparent brown colour [10] (Fig. 1a). BAT, which is found in a limited number of areas in the human body such as the neck region, collarbones, shoulder blades and inter-shoulders, is close to brown in colour due to its high vascularization and mitochondrial content. The amount of BAT in the human body generally decreases with age while the amount of WAT increases [31,32]. Brown adipocytes display a high metabolic activity characterized as "mitochondrial uncoupling" [10]. These cells contain numerous, specialized mitochondria which oxidize fat and carbohydrates for heat generation. This metabolic process is due to the presence of "uncoupling protein 1" (UCP1) that is highly expressed in brown adipocytes and participates in oxygen uptake, caloric expenditure and body temperature regulation [33,34]. In fact, it is a proton carrier located in the inner mitochondrial membrane of brown adipocytes which catalyzes proton leaks across the membrane and thus uncouples it from oxidative phosphorylation in ATP production, providing thermogenesis [33–35]. It therefore plays a vital role in the prevention of hypothermia in mammals exposed to the cold [36–38]. There are various studies in the literature showing that regular exercise induces the expression of UCP1 for regulation of both body temperature and metabolic[36,39–41]. Therefore, brown adipocytes have a significant capacity to consume calories. Accordingly, BAT is thought to have therapeutic potential for the treatment of metabolic diseases such as obesity and type 2 diabetes mellitus (T2DM), common diseases worldwide caused by a deterioration in the energy balance of the body [9,42]. Although autologous BAT transplantation in small animal models is reported to contribute to metabolic improvement in studies conducted to increase BAT, its application in humans is unfeasible since the sources of human BAT are limited [43]. The amount of BAT in adults was once considered to be negligible but studies conducted in recent years have refuted this view and revealed the existence of active BAT in adult humans [36].

1.1.3. Beige adipose tissue

In addition to brown adipocytes, which are located in anatomical BAT depots, another cell type with thermogenic activity is “beige” or “bright” adipocytes (Fig. 1b). These cells may appear in the anatomical regions of WAT after thermogenic stimuli. They have a white and adipocyte-like phenotype, and when induced, they acquire a brown-like phenotype, leading to increased thermogenesis. This process is called “browning” and can occur by two different mechanisms: White to brown transdifferentiation of adipocytes or induction of adipocyte progenitor cell differentiation [44,45]. Browning generally occurs in subcutaneous fat deposits and requires the expression of many transcription factors involved in thermogenesis, such as PRDM16, PPAR-γ and UCP1 [46]. There is no evidence that the thermogenic function of beige adipocytes is ultimately different from classical brown adipocytes, but various *in vivo* and *in vitro* studies have suggested that beige adipocytes may also be effective in the treatment of obesity and related comorbidities [46–49].

1.1.4. Yellow adipose tissue

In addition to WAT and BAT, there are also two further AT types defined according to their different characteristics. Yellow adipose tissue (YAT) (Fig. 1e) is also known as bone marrow adipose tissue (bMAT) and has some common properties related to WAT and BAT [50]. YAT not only stores triglycerides, but also plays a role in systemic energy regulation and insulin sensitivity. In addition, it contributes to raised serum levels of adiponectin during caloric restriction as an endocrine organ [51]. During normal aging processes, healthy and haematopoietically active red bone marrow is replaced by YAT [50]. In the case of obesity, the amount of both WAT and YAT increases in the body. However, in cases of hunger and anorexia, the amount of YAT increases while WAT decreases [52].

To date, only a few 3D *in vitro* YAT models have been reported. In one of these studies, human and mouse-derived bone marrow stem cells (bMSCs) were seeded on silk scaffolds and stably cultivated for 3 months with good cell viability and adipogenesis.

This journal is © The Royal Society of Chemistry 20xx

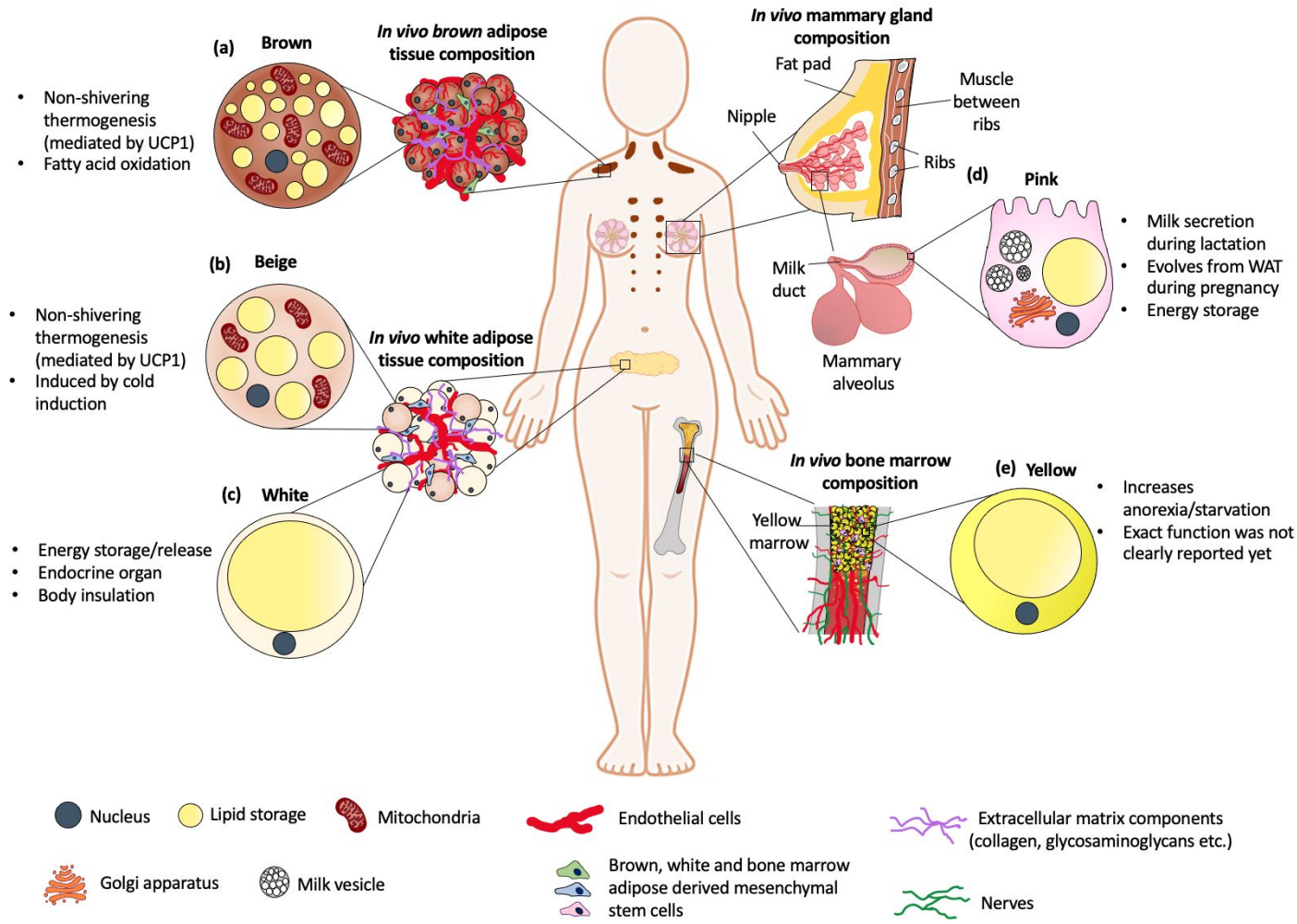

Fig. 1. There are five types of adipocytes with different functional and morphological characteristics in the body: Brown, beige, white, pink and yellow. (a) Brown adipocytes are the main cells that contain small lipid droplets in their cytoplasm, highly express UCP1 protein and are responsible for thermoregulation. They are found at specific areas in the body such as the shoulder blades, neck region, collarbones, and around the vertebrae. (b) Beige adipocytes are generally stored in white adipose tissue depots and play a role in thermoregulation by acquiring a brown-like phenotype when induced. (c) White adipocytes are the main cells of white adipose tissue, which have a high energy storage and release capacity, and perform an endocrine function by producing various adipokines. (d) Pink adipocytes are responsible for secreting milk during pregnancy and lactation and are cells formed by the reversible conversion of white adipocytes in the mammary glands. (e) Yellow adipocytes are cells located in the bone marrow of the body and are involved in systemic energy regulation.

Furthermore, it was reported that when myeloma cells were co-cultured in 3D, undifferentiated stromal cells decreased and delipidation occurred in adipocytes. It was noted that the proposed model could be used for investigation of bone marrow diseases and biological processes, drug discovery, and specific signal research [53].

In another study, Ravichandran et al. designed a bMAT analogue made of GelMA (gelatin methacryloyl) hydrogel/medical grade polycaprolactone (mPCL) scaffold composite to model the bone marrow microenvironment and examine the effects of biomechanical stimuli on the bone marrow niche and AT. GelMA hydrogels obtained by photocrosslinking were designed to be within the lumen of melt electro-written (MEW) mPCL scaffolds to recapitulate the bone marrow microenvironment. In addition, a bioreactor was used to examine the effects of mechanical loading on the model. Compression loading (1 Hz, 2 h/day, 3 days/week, 3 weeks) applied with the bioreactor for 3 weeks increased the proliferation and lipid accumulation of bone marrow stem cells compared to unloaded controls, and was reported to cause a significant decrease in adipokine secretion [54].

1.1.5. Pink adipose tissue

Pink adipose tissue (PAT) occurs when white adipocytes in the mammary glands are reversibly converted to milk-producing glands during pregnancy, lactation, and post-lactation [55]. Alveolar mammary cells are also defined as pink adipocytes since this type are parenchymal cells of AT, characterized by a large number of cytoplasmic lipids, and the colour of this AT is pink during pregnancy [56] (Fig. 1d). Although transformation of white or brown adipocytes into alveolar cells has been reported in 2D cultures [55], a 3D *in vitro* PAT model has yet to be developed.

1.2. Importance of vascularization in adipose tissue

1.2.1. Development of highly vascularized tissue

AT, one of the main regulators of whole-body metabolism, is heavily vascularized to maintain metabolic functions and homeostasis [57,58]. In general, vasculogenesis and angiogenesis are defined as the main mechanisms by which new blood vessels are formed. Vasculogenesis is the differentiation of progenitor cells (angioblasts) into endothelial cells (ECs) and the *de novo* formation of a primitive vascular network [59]. Angiogenesis, on the other hand, involves the expansion of new vessels from an existing vascular network, where EC growth, migration, polarization, sprouting, and lumenization lead to the formation of a functional circulatory system, along with the growth of new capillaries from pre-existing blood vessels [18,59]. AT is highly vascularized, and all adipocytes are in contact with at least one blood vessel. This vascularization is created during AT development in the embryo. Therefore, as a highly vascularized tissue, a functional vascular system is crucial for AT in terms of supplying oxygen, nutrients, hormones and growth factors, and to maintain homeostasis [60].

Adipocyte differentiation and AT growth depend on new vessel development for efficient nutrient and oxygen delivery. During adulthood, the AT has the ability to expand multiple times, and the expansion of the tissue necessitates adequate vascularization to allow proliferation of cells. Vascularization in AT develops through angiogenesis, in which new blood vessels develop from pre-existing blood vessels in the tissue [61]. Moreover, angiogenesis plays a complex role in obesity in terms of promoting the disease [57].

1.2.2. Cross-talks between adipocytes and endothelial cells for adipose tissue homeostasis

In AT, mature adipocytes, the most prominent cell type of the tissue, are in direct contact with EC via cellular crosstalk, thus forming the vascular structure [17,62]. Accordingly, the homeostasis of AT and the associated degree of vascularization are mainly provided by adipocytes, preadipocytes, and ECs [17]. Both ECs and adipocytes secrete VEGF (vascular endothelial growth factor), which acts in angiogenesis by promoting EC migration and proliferation [62].

In fact, VEGF is the master regulator of angiogenesis. However, other cells of the AT also affect angiogenesis and vasculogenesis [57]. Preadipocytes are effective in EC migration, as PPARγ and leptin are upregulated and angiogenesis is stimulated when these cells differentiate into adipocytes. In addition, VEGF-A upregulation in adipocytes promotes vascularization and induces AT "browning" with UCP1 and PGC1α (PPAR gamma coactivator 1 alpha) upregulation [63]. Moreover, upregulation of adiponectin secreted by adipocytes in this process is also effective in angiogenesis [62]. Accordingly, the complex crosstalk between these two cell types is important in terms of supporting both AT balance and the vascular system [20]. Furthermore, EC-adipocyte co-cultures cause proliferation of both cell types and adipocyte differentiation, but direct contact of mature adipocytes and ECs may cause dedifferentiation of adipocytes into preadipocytes [62,64]. However, recent studies conducted by our research group have shown that mature adipocytes are still maintained after the addition of blood vasculature [65]. Various studies have indicated that ECs reduce the differentiation of preadipocytes and increase their proliferation [66,67]. Moreover, adipose-derived mesenchymal stem cells (ADSCs) are another potential cell source for vascularized AT production, as they are ubiquitous, and can differentiate into both adipocytes and ECs *in vitro* [19]. In a related report, ADSCs and HUVECs were co-cultured to produce differentiation in the adipocyte lineage as well as angiogenic structures [68].

In general, inducing adipogenesis and angiogenesis simultaneously in vitro is challenging so co-culture studies performed directly with differentiated adipocytes can be more advantageous. In addition, some studies make sequential differentiations to avoid this problem [62,69,70].

2. Materials for vascularized adipose tissue reconstruction

Studies conducted on tissue engineering using various natural and synthetically derived polymers are extremely promising in terms of reconstructive and plastic surgery [71,72]. The development of bioactive structures capable of regenerating AT has made great progress towards addressing the limitations of current treatments, but their lack of vascularization and the ability to meet the important size requirements of tissue defects limit their clinical use [73]. Nevertheless, these studies can help to clarify the origin and progression mechanism of diseases, as well as being used for therapeutic screening and as diagnostic tools [74]. In addition, the developed approaches can guide the understanding and regulation of adipogenesis to recapitulate the impact of cell-ECM interactions and the development of new biomaterials for obtaining vascularized AT in a prevascularized way or by neovascularization following implantation.

2.1. Natural components

Numerous WAT engineering studies using naturally sourced polymers can be found in the literature. Collagen [75–77], gelatin [78], silk [79], fibrin [80,81], Matrigel™ [82–85], and hyaluronic acid [86] are examples of natural origin polymers most commonly used for WAT engineering. In addition, studies performed with decellularized ECM also have a large place in the literature [87–91]. Table 1 presents some examples of the published natural scaffolds for *in vitro* AT reconstruction. We discuss the studies in which vascularized AT structures were biofabricated with these materials below.

2.1.1. Collagen

Collagen is one of the most common natural polymers and is widely used in AT regeneration. It is readily available, has well-established biocompatibility, and can support cellular ingrowth and new matrix synthesis [92]. It constitutes 25-35% (by dry weight) of natural AT-ECM [1]. To date, in studies conducted with collagen matrices, successful results have been obtained in the stimulation and adipogenic

 This journal is © The Royal Society of Chemistry 20xx

differentiation of preadipocytes and stem cells [93–95]. Collagen gels not only facilitate cell adhesion [96] or mechanically support cells but also promote adipocyte growth. Indeed, collagen biologically supports tissue formation as it is one of the main components of the ECM. Therefore, it not only offers a physical environment for cell survival, but also provides a suitable niche for cell attachment, differentiation and new ECM formation [95].

Concerning the angiogenic potential of collagen, it has been shown that collagen matrices can support neovascularization in 3D-cell culture models containing human preadipocytes [76,95]. After 3, 8, and 12 weeks, *in vivo* layers of AT with new vessels and rich vascularization were obtained. However, collagen only has limited angiogenic induction with about 15-20% of fully vascularized explants after 12 weeks *in vivo,* requiring a longer *in vivo* evaluation. Hardening or thickening of the outside of the scaffold, and thus calcification or loss of thickness, are also common adverse outcomes which affect the implant supply of nutrients and oxygen [75,95]. Moreover, Von Heimburg et al. showed that pore sizes between 65 and 100 µm were advantageous for good cell distribution for preadipocyte development and growth in sponge-formed collagen scaffolds obtained by lyophilization [95].

A recent study showed that microvessels that expand through angiogenesis in an organoid model composed of microvascular fragments with MSCs and adipocytes derived from MSCs expand when placed in a 3D collagen matrix. In organoids placed in collagen after day 2 or 5 of culture (3 mg/ml), the collagen itself was not essential for vascular formation, but it caused an increase in vessel diameter in the organoids [97].

Chemical or physical crosslinking of the collagen affects both vascular network formation and tissue regeneration. In a related study, Chuang et al. compared physically and chemically crosslinked injectable collagen matrices in terms of AT regeneration and vascular network formation. They showed that chemically crosslinked collagen which was obtained from the covalent crosslinking of the side chains induced by one-step enzyme mediation in an aqueous solution showed successful results in nude mice with encapsulated human ECFCs (endothelial colony forming cells) and bone marrow MSCs in terms of mature adipocyte formation (94% area of a construct) with a vascular structure [77]. As a result, modification of the polymerization method can improve both tissue regeneration and vascular formation.

2.1.2. Fibrin

Fibrin gel, which is an ideal carrier in tissue engineering studies due to its biocompatible, biodegradable and non-toxic properties, is generally used as a matrix or carrier for cells in *in vivo* AT engineering studies [80,81]. When mixed with preadipocytes, implantation into rat showed a vascular supply establishment after 2 weeks, and the volume was retained 1 year after implantation with robust lipid structures of healthy appearance [80]. In another *in vivo* study with preadipocytes suspended in a fibrin matrix, the suspension was implanted subcutaneously into the chorioallantoic membrane (CAM) of fertilized White-Leghorn eggs and vascularization was observed after 8 days [81]. Torio-Padron et al. confirmed both adipogenesis and angiogenesis in implanted fibrin gels containing human preadipocytes in nude athymic mice. A dense vascular structure was observed and the newly formed AT persisted for at least 9 months after transplantation? [98].

When mixed with collagen in the form of collagen microfibers (CMF), fibrin gel helps to regenerate the vascularized structure of AT prior to implantation using human mature adipocytes, ADSCs and HUVECs [99], with a higher cell viability (84±6%) and volume maintenance than with non-prevascularized tissue implantation or classic lipoaspirate tissue implantation. Although fibrin matrices have generally been shown by various groups to induce vascularization *in vivo*, their effect on adipogenesis is limited and their dehydration and degradation, when used alone, limit their use in long-term cell culture research [100].

2.1.3. Matrigel™ and Myogel

Matrigel™ is a commercially available product derived from mouse sarcoma and is a mixture of various basal membrane proteins (collagen type IV, laminin…) [83,101]. According to various studies conducted with preadipocyte cell lines *in vitro* [82,83], or subcutaneous injection into rat or mouse models *in vivo* [85,102]. Matrigel™ is a material which can be used for AT formation, as well as for supporting or inducing neovascularization [82,83,85,103]. However, since it is a tumour-derived xenogeneic material, its direct clinical use has limited potential [101]. In this context, an alternative can be Myogel, a material extracted from the skeletal muscle of various animal species. It contains laminin isoforms distinct from Matrigel™ and has been found to support preadipocyte differentiation *in vitro* and vasculature formation when implanted *in vivo*, recreating a vascularized AT without the addition of exogenous growth factors. [104].

2.1.4. Alginate

Alginate alone is not suitable for cell attachment or growth, and cannot be degraded by cells. It can therefore be modified in various ways including peptides or RGD ligands to induce vascular network formation [100] or for AT engineering research [105]. By using alginate hydrogel whose polymer chains are sensitized to hydrolysis by partial periodate oxidation to encapsulate ADSC, Kim et al. also confirmed the induction of adipogenic differentiation *in vitro*, and then newly formed vessel formations in a large amount of reconstructed AT *in vivo* in nude mice after 10 weeks. However, it was stated that additional studies are required to examine the vascularization kinetics [106].

2.1.5. Hyaluronic acid

Hyaluronic acid (HA), one of the important components of the ECM, is a polysaccharide composed of repeating disaccharide units of D-Glucuronic acid and N-acetyl-D-glucosamine linked by alternating (1→4) and (1→3) bonds [107,108]. Due to its high water retention and intrinsic swelling properties, HA induces cell attachment and

migration, while being beneficial for AT development [107–109] as well as supporting both adipogenesis and neovascularization *in vivo* [86,110].

HA modified scaffolds can also be beneficial. In a study using HYAFF11, an esterified form of hyaluronan, (specifically, where the carboxylic function of the monomer glucuronic acid in the hyaluronic acid chain was esterified with benzyl groups) loaded with human preadipocytes and implanted into nude mice, it was reported that blood vessel formation occurred after 3, 8 and 12 weeks. However, the scaffold pore size decreased during the implantation period, limiting the adipogenic differentiation [86]. Other chemically modified HA-based hydrogels have also led to efficient vascularization results with [111] or without AT development [112] in various tissue engineering studies. However, these chemical modifications might cause toxicity, limiting their use *in vivo* [100].

2.1.6. Decellularized matrices

Decellularized mammalian tissues used as a tissue scaffold can be degraded in the body and support matrix remodelling [87]. Materials derived from decellularized ECM can mimic the body's natural environment, triggering normal cellular organizations and behaviours. In addition, decellularized tissues have several advantages in terms of biodegradability and biocompatibility [113] but the difficulty in preparation of decellularized matrices limits their widespread use.

Decellularized biomaterials such as decellularized human placenta, human AT, or porcine AT have been used by various research groups for WAT production [87–89,102,111,114,115]. In various 3D *in vitro* culture studies with human ADSCs and matrices derived from decellularized AT, the latter has been shown to strongly support adipogenesis and also be adipoinductive [88,90,114–116]. Moreover, AT models obtained from these scaffolds also support neovascularization with adipogenesis when implanted or injected subcutaneously in rodents [88,114].

As each tissue has its own unique complex composition and concentration of chemical components in its ECM elements, known to regulate numerous cell processes, including attachment, survival, migration, proliferation, and differentiation, it can be thought that the use of AT as a decellularized matrix for 3D AT production would be more advantageous in terms of AT regeneration [115].

In a recent study, a rat decellularized lung matrix (DLM) was used due to its advantages such as having a preserved acellular vascular bed allowing effective graft perfusion and pre-vascularization, and allowing high density adipose filling (Fig. 2a-c). Adipocytes were loaded through the trachea, while HUVECs were loaded through the alveolar pulmonary artery of the DLM. Samples harvested at the end of the 7th day showed that the adipocytes were distributed throughout the entire DLM structure, and filled the branches forming the vasculature tree with internal branching (Fig. 2b,c). Although this is a promising approach for AT regeneration, it has several restrictions such as the fact that different lobe sizes may limit parallel studies or that time points are limited by the number of lung lobes [117].

2.2. Synthetic components

Although synthetic biomaterials are generally biologically inert, the advantages of these materials are that they can offer results which are more predictable, while a uniform structure can be obtained in repetitive solutions and different derivatives tailored for specific applications [118]. Biodegradable synthetic polymers are frequently used in tissue engineering applications, and especially in AT engineering applications, because of their superior chemical and mechanical properties and controlled degradability, compared to natural polymers [12]. They are effective for adipocyte proliferation and migration [15] as well as for the production of AT substitutes *in vitro* and *in vivo* when used with adipogenic stimulants [119,120]. Thus, AT related studies conducted with different synthetic scaffolds such as poly(caprolactone) (PCL) [121], poly(ethylene glycol) (PEG) and derivatives [122,123], and poly(ethylene terephthalate) (PET) [124] can be found in the literature. The synthetic polymers allowing the generation of vasculature formation in AT engineering studies are briefly discussed below.

2.2.1. Poly(glycolic acid) (PGA)

PGA is a widely used material in medicine, especially in surgical suture material, due to its good degradation behavior in vivo 125. PGA fiber meshes have been used in differentiation of adipocyte precursor cells into mature adipocytes and as a cell-supporting material in long-term *in vitro* culture conditions [126,127]. Fischbach et al. showed that when loaded with 3T3-L1 preadipocytes and implanted into immunodeficient mice, predifferentiated tissues *in vitro* resulted in fat pads histologically comparable to natural fat with neovascularization *in vivo* within 3 weeks and with lumen formation and angiogenesis occurring from the second month after implantation [126]. In another study, Lin et al. obtained a 3D culture by seeding human ADSCs into a structure consisting of a PGA sheet, gelatin sponge and poly(propylene) (PP) mesh. The resulting constructs were implanted into a mouse model and growing blood vessels with newly formed AT were observed for *in vivo* samples collected at the end of 2, 4 and 6 months [128]. Despite these examples, PGA is a rapidly degrading polymer known for its hydrolytic instability. Also, the increase in glycolic acid resulting from degradation carries the risk of creating an undesirable immune response, thus limiting the clinical use of PGA [129].

2.2.2. Poly(lactic acid) (PLA)

In AT engineering, PLA is another aliphatic polyester used in different forms such as nanofibers [130] or 3D printed scaffolds [131]. When implanted in rats for 12 months, with or without filling with a collagen type 1 hydrogel, the 3D printed PLA frame with a size of 6 × 6 × 3 mm^3 maintained its shape and all implants showed new AT formation and were covered with a microvascular network [131]. However, PLA has some important disadvantages that limit its use, such as biological inertness, low cell attachment, low degradation rate, and acid degradation by-products [132].

This journal is © The Royal Society of Chemistry 20xx

In all the scaffold-based approaches mentioned above, the materials of both natural and synthetic origin have various merits and demerits in terms of tissue engineering. However, although synthetically derived scaffolds have various advantages such as being easy to process, able to be produced in a certain shape and geometry, and have limited variability between different production batches, they have important disadvantages. These include the inability to show biocompatibility comparable to naturally derived scaffolds due to the possibility of degradation products causing undesirable immune responses or the possibility of changing the local microenvironment in vivo. On the other hand, naturally derived scaffolds are not mechanically strong, but have several important advantages. Because they can easily incorporate the tissue microenvironment and mimic the natural ECM structure and composition, as well as being oxygen permeable and highly biocompatible, the use of adipoinductive and vascular-supporting materials, such as collagen and fibrin, may lead to more advantageous results in soft tissue engineering.

2.3. Scaffold-free vascularized adipose tissue engineering

Techniques such as magnetic levitation cultures [133], hanging drop [134] or the liquid overlay method [135] are biomimetic tissue production approaches which are performed by gaining spheroid formation to cells without using a polymeric tissue scaffold. In this way, 3D intercellular signalling and AT organogenesis can be recapitulated and since they do not contain any external material, these models can be advantageous for *in vivo* transplantation applications [136]. However, while scaffold-free systems are generally superior to scaffold-based systems in terms of biocompatibility, the latter allow better manipulation of attributes such as position, geometry, and size [137]. Daquinag et al. conducted a 3D magnetic levitation culture study to model the development and growth of WAT in organoids they called “adipospheres”, using 3T3-L1 and murine endothelial cell line bEND.3 cells. In these tissues, the cells remained viable for a long culture period with lipogenesis and also led to a vascular-like network assembly [138]. Muller et al. developed a vascular structure with adipose progenitors and self-assembled endothelial cells derived from the stromal-vascular fraction of human subcutaneous WAT in the adipose spheroid culture they developed, showing a vascularized organization and mature adipocytes containing unilocular lipid vacuoles (Fig. 2d-f) [139]. The obtained spheroids were injected into immunodeficient mice and after 7 days of implantation, human ADIPOQ and PPARγ gene expressions by RT-PCR analysis revealed that there were still human adipocytes within the vascularized spheroids thanks to their integration into the host vascular structure (Fig. 2f).

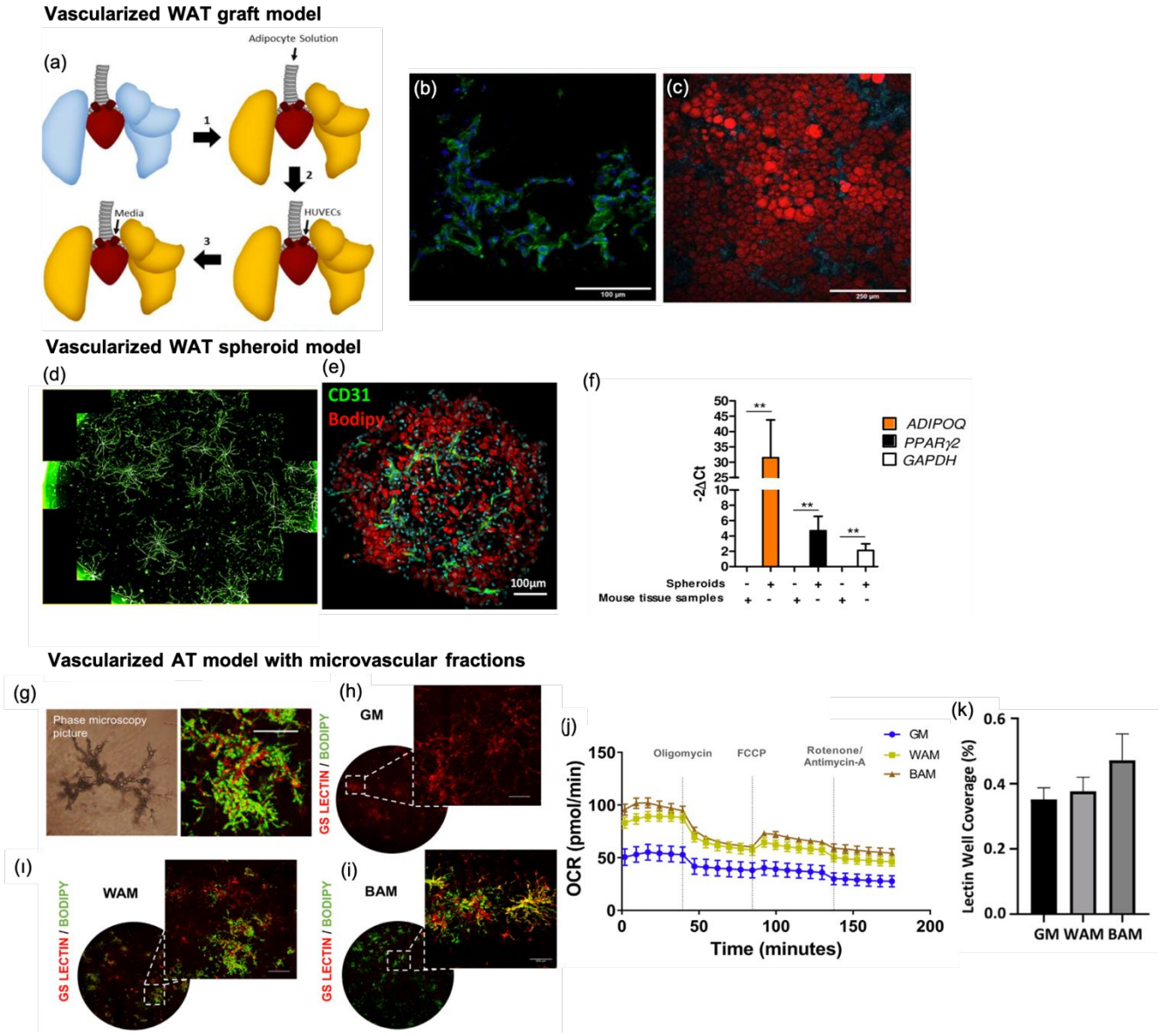

Fig. 2. Various *in vitro* 3D vascularized adipose tissue approaches. (a-c) Vascularized WAT graft model by using decellularized lung matrix (DLM). (a) Schematic representation of cell seeding onto DLM. Step 1: The DLM was recellularized with adipocyte solution through the trachea. Step 2: The vasculature was recellularized with HUVECs through the pulmonary artery. Step 3: The lung was placed in a custom bioreactor and perfused with the media through the pulmonary artery. (b) Endothelial only seeded DLM (blue-nuclei, green-endothelial cell) showing a network of endothelial cells. Scale bar = 100 µm. (c) Tile scan of entire left lobe (red adipocytes, teal-endothelial cells, blue-nuclei). Image shows that adipocytes seeded through the trachea remain in the inner portion of the lobe and are surrounded by the endothelial cells seeded through the vasculature. Scale bar = 250 µm. (n = 1). (This content is shown under the Creative Commons Attribution 4.0 International License (CC BY 4.0); adapted from reference 117). (d-f) Vascularized WAT spheroid model. Vascular structure of WAT spheroids comprising adipose progenitors and self-assembled endothelial cells derived from the stromal-vascular fraction of human subcutaneous WAT. (d) Endothelial networks visualized by CD31 staining; the whole surface of a well was scanned using the OperettaTM screening system. (e) BODIPY staining for lipid vesicles and CD31 immunostaining for vascular structure spheroids. (f) Human adipocytes remaining in spheroids were revealed by assessing the expression of the human adipocyte-specific markers ADIPOQ and PAPRγ2 by qRT-PCR. Mouse tissue samples were tested to highlight the human specificity of the primers used. Data are mean ± SEM. **p < 0.01. (This content is shown under the Creative Commons Attribution 4.0 International License (CC BY 4.0); adapted from reference 139). (g-k) Vascularized beige adipose tissue model using human microvascular fraction (hMVF). (g) Representative phase microscopy image and higher magnification image of stained hMVFs after differentiation. Scale bar = 12 µm. (h-i) Representative confocal images of hMVF grown in fibrin scaffolds and stained with GS-Lectin I (red) to visualize vascular network formation and BODIPY (green) to identify the presence of lipid droplets cultivated in growth medium (GM), WAM (white adipogenic differentiation medium) and BAM (beige adipogenic differentiation medium). Scale bars = 200 µm. (j) Oxygen consumption rate (OCR) tracing of microvascular fragments cultivated in GM, WAM and BAM. (k) Quantitative analysis of vessel formation as determined with lectin accumulation. (This content is shown under the Creative Commons Attribution 4.0 International License (CC-BY 4.0); adapted from reference 187).

This journal is © The Royal Society of Chemistry 20xx

Table 1. Materials used for WAT reconstruction

Material	Cell Used	Prevascularization *in vitro*	Neovascularization *in vivo*	Remarks	References
Collagen type I	Rat and human mature adipocytes	No	No	Unilocular, multilocular adipocytes and fibroblast-like cells	140
	Human preadipocytes	No	Yes	Adipogenesis and vasculogenesis occurred after *in vivo* implantation	75
	Human preadipocytes	No	Yes	Adipogenesis and vasculogenesis occurred after *in vivo* implantation	95
	Human bone marrow MSC	No	No	Adipogenesis and membrane-free lipid vacuole formation *in vitro*	93
	hMSC, MDA-MB-231, HEK293T	No	No	Recapitulation of breast cancer tumor microenvironment	141
	hADSC, Mouse mature adipocytes	No	No	Adipogenesis in 3D culture	142
	Human mature adipocytes, hADSC, HUVEC	Yes	No	Adipogenesis and vasculogenesis *in vitro* after 7 days of culture	143
Gelatin	Human bone marrow stromal cells	No	No	Adipogenesis in 3D culture	144
	Human ADSC	No	Yes	Adipogenesis and vasculogenesis occurred after *in vivo* implantation	145
	Human MSC	Yes	No	Prevascularized channels formed with sacrificial alginate templates within gelatin sponge scaffolds	146
Methacrylated gelatin	Human bone marrow MSC	No	No	Adipogenesis in 3D culture	147
	Human mature adipocytes	No	No	Volume stable 3D mature adipocyte culture	148
	Human ADSC	No	No	Adipogenesis on 2D culture	149
Collagen and Gelatin	Human preadipocytes	No	Yes	Adipogenesis and vasculogenesis occurred after *in vivo* implantation	78
	Human preadipocytes	No	Yes	Adipogenesis and vasculogenesis occurred after *in vivo* implantation	150
Silk	Human BMSC, Human ADSC	No	No	Adipogenesis occurred in 3D culture and *in vivo* implantation	151

ARTICLE

Table 1. *(Continuous)*

	Human ADSC, HUVEC	Yes, 7th and 14th cultures	No	*In vitro* adipogenic differentiation and vasculogenesis	68
	Human ADSC, endothelial cells	Yes	No	*In vitro* adipogenic differentiation and vasculogenesis	79
	Human liquefied AT	Yes	No	Long-term (3 months) explant culture	152
Fibrin	Rat preadipocytes	No	Yes	Adipogenesis and vasculogenesis occurred after *in vivo* implantation	81
	Human preadipocytes, Human dermal microvascular endothelial cell	Yes	No	*In vitro* angiogenesis	66
	Human preadipocytes	No	Yes	Adipogenesis and vasculogenesis occurred after *in vivo* implantation	98
	Rat microvascular fragments	Yes	No	*In vitro* adipogenic differentiation and angiogenesis	47
Matrigel	3T3-F442A preadipocytes	No	Yes	Adipogenesis and vasculogenesis occurred after *in vivo* implantation	83
	Human mature adipocytes	No	Yes	Vasculogenesis occurred after *in vivo* implantation	85
Alginate	Human ADSCs	No	Yes	Adipogenesis and vasculogenesis occurred after *in vivo* implantation	106
Hyaluronic Acid	Human preadipocytes	No	No	*In vitro* adipogenic differentiation	110
	Human preadipocytes	No	Yes	Adipogenesis and vasculogenesis occurred after *in vivo* implantation	86
	Inguinal fat pad	No	Yes	Adipogenesis and vasculogenesis occurred after *in vivo* implantation	153
Collagen/Hyaluronic Acid	3T3-L1 preadipocytes	No	No	*In vitro* adipogenic differentiation	107
Gelatin/Hyaluronic Acid	Porcine ADSCs	No	Yes	Adipogenesis and vasculogenesis occurred after *in vivo* implantation	108
Decellularized human placenta	Human adipose precursor cells	No	No	*In vitro* adipogenic differentiation	87

Table 1. *(Continuous)*

Decellularized human AT	hADSCs	No	Yes	Adipogenesis and vasculogenesis occurred after *in vivo* implantation	88
	hADSCs, rat ADSCs	No	Yes	Adipogenesis and angiogenesis occurred after *in vivo* implantation	90
Decellularized apple plant	3T3-L1	No	No	*In vitro* adipogenic differentiation	154
PGA	Rat ADSCs	No	No	*In vitro* and *in vivo* adipogenic differentiation	120
	3T3-L1 preadipocytes	No	No	*In vitro* adipogenic differentiation	155
	3T3-L1 preadipocytes	No	Yes	*In vitro* adipogenic differentiation. Vasculogenesis occurred after *in vivo* implantation	127
PLA	Human bMSCs	No	No	*In vitro* adipogenic differentiation	130
PLGA	Rabbit bMSCs	No	No	*In vitro* and *in vivo* adipogenic differentiation	156
	Rat bMSCs	No	No	*In vitro* adipogenic differentiation	157
	Human ADSCs	No	No	*In vitro* and *in vivo* adipogenic differentiation	158
	Human ADSCs	No	No	*In vitro* adipogenic differentiation	119
PEG	3T3-L1 preadipocytes	No	No	*In vitro* adipogenic differentiation	122
PEGDA	Human bMSCs	No	No	*In vitro* adipogenic differentiation	123
PET	3T3-L1 preadipocytes	No	No	*In vitro* adipogenic differentiation	124

3. Applications for organs or diseases reconstruction

3.1. Drug screening models against obesity and diabetes

Today, there are various approaches for drug screening and discovery studies by morphological and functional 3D modelling of AT. These can be classified as 3D AT constructs obtained using tissue scaffolds [159], scaffold-free adipose spheroids [160], or "adipose-on-chip" models [161,162] performed with organ systems on a chip, which is an innovative approach in drug screening research. These systems are promising for researching WAT biology, examining pathophysiological mechanisms such as obesity and diabetes, and drug R & D applications. Because human cells respond differently to drugs, animal models cannot fully reproduce human AT, which leads to a high failure rate. Even using human cells, in vitro models in 2D cannot reproduce adipocyte physiology and 3D models using patients' cells are required for more accurate responses. 'The path to US Food and Drug Administration (FDA) approval for a new drug is long and troublesome, a process usually lasting more than 10 years with a cost of $2.8 billion and a success rate of only ~10% [163].

In addition to these studies, organ-on-chip systems have become important in the investigation of complex biochemical processes such as drug screening and organ modelling in recent years. These platforms allow tissues to be integrated into vasculature-like microfluidic perfusion chambers [113,162] modelling paracrine signals and adipocyte functions, which have good potential for drug screening studies for AT [162]. With these models, the dose dependent effect of lipid droplet inhibition activity in the presence of anti-obesity agents, for instance Orlistat and Quercetin, can be assessed in 3T3-L1 cells [164]. Also, Rogal et al. presented a system that integrates human primary mature adipocytes into a perfused microfluidic chip with their WAT on chip system, where basic and physiological cellular responses as well as drug responses can be monitored [162]. Yang et al. designed 3D adipose microtissues by differentiating human-derived ADSCs into mature adipocytes in a microfluidic system. It was stated that this system, which investigates AT response under interstitial shear stress at the physiological level, could serve as an *in vitro* drug testing tool for adipose-related diseases [165].

However, the above models cannot recapitulate the important cell-cell interaction occurring in AT between adipocytes and ECs. To at least reproduce it indirectly, "organ-on-a-chip" systems showing multi-organ chips have great potential [166]. This is a promising alternative to animal models, including a physiological microenvironment with vasculature-like microfluidic perfusion and a more accurate simulation of cell matrix interactions [167]. Recapitulating the vasculature is a further step up to more reliable AT models but the regeneration of a disease-related model using patient cells or recreating their phenotype is also important for drug screening assessment.

Obesity, another metabolic disease, defined as a body mass index of 30 kg/m^2 or more, is characterized by fat accumulation resulting in chronic inflammation in metabolic tissues [168]. T2DM, which is frequently observed due to obesity and physical inactivity, is characterized by insulin resistance (IR) and pancreatic β-cell dysfunction in peripheral tissues. IR is the inability of the insulin secreted by the pancreas to produce the necessary or sufficient response in fat, muscle and liver cells. Overall, obesity is characterized by an excessive increase in AT, often accompanied by IR and T2DM [169]. Obesity is characterized by the accumulation of fat in metabolic tissues in chronic inflammation and increased adipocyte cell death [170]. Thus, in the case of obesity or diabetes, confirming IR or AT inflammation are important factors for developing physiologically appropriate AT models for the controlled examination of both normal and diseased functions of these comorbidities. These examinations might lead to an understanding of the stages of the disease and the processes related to fat metabolism and hence to therapeutic solutions [168].

Moreover, during the obesity state in addition to adipocyte enlargement, macrophage accumulation is promoted [171], aggregating around dead adipocytes with a view to removal of cytotoxic residues [172]. While macrophage infiltration is increased in WAT during obesity, its interaction with adipocytes, inflammatory and EC interactions pathways has been extensively studied as it plays an important role in reprogramming WAT metabolism and identifying therapeutic targets to ameliorate obesity and metabolic disease [173]. In summary, three systems are thus required to properly model AT biology: vasculature, adipocytes and immune cells.

Based on IR, Choi et al. examined the effect of high insulin exposure in a 3D adipocyte-EC co-culture with a 2D adipocyte monoculture and silk fibroin scaffold prepared by a salt leaching method with 500-600 μm pore size. Cells were cultured at normal (1 μM) or high insulin concentration (10 μM), and the ability of the 3D system to elicit a physiological response to hyperinsulinemia was higher than the 2D cultures. The addition of endothelial cells to the system has played an important role not only in physiologically mimicking the tissue *in vivo*, but also in the generation of relevant responses in the case of hyperinsulinemia of ECs. This is because endothelial dysfunction, which is characterized by the decrease in nitric oxide bioactivity observed in the IR state, is closely related to the secretion of proinflammatory cytokines from AT and increased free fatty acid levels. Therefore, it can be concluded that the presence of ECs in co-cultures contributes to the hyperinsulinemic effect in a similar manner to that *in vivo* [174].

However, the above system still lacks vascular structures. To actually add the ECs interaction, Louis et al. developed a drug screening model that mimicked the physiology of patients' Body Mass Index (BMI) by encapsulating human mature adipocytes into CMFs from collagen type I, the most prevalent ECM component in AT, to recapitulate adipocyte functions and *in vivo* physiology together with the addition of blood vessels [65] (Fig. 3a-c). To assess adipose drops, mature adipocytes were mixed with CMF and embedded in fibrin gel. This model provided a realistic high-throughput fat-targeted drug screening model for obesity or diabetes and shows a wide range of measurable functional outcomes. The addition of vascularization to the system provided a higher maintenance of mature adipocyte metabolism, while the

 This journal is © The Royal Society of Chemistry 20xx

crosstalk between the blood vessel vasculature and adipocytes in the drop could be modelled. In detail, during preadipocyte differentiation, upregulation of PPARγ and leptin stimulates angiogenesis. Furthermore, co-culture of HUVECs and differentiated adipocytes is known to show a vascular network organization supported by upregulation of vascular endothelial growth factor (VEGF) and leptin secretion from adipocytes. By maintaining this crosstalk in the vascularized adipose drop tissues, this model was able to reproduce the lower BMI-dependent leptin regulation in mature adipocytes following the increase in the obesity phenotype.

There are actually few studies that include all three systems of vasculature, adipocytes and immune cells. Huttala et al. studied the effect of macrophages on adipogenesis and protein secretion in their model developed using human adipose stromal cells (hASC), ECs and monocytes/macrophages in a 2D *in vitro* cell culture. It was reported that lipid accumulation was higher in adipocytes in the presence of macrophages and protein secretion was more affected by macrophages when vasculature was not present compared to the mild effect when vasculature was present. For this reason, the presence of vascular structures may lead to more appropriate intervention methods in investigating obesity-related comorbidities associated with vascular change and inflammation [171]. Additionally, Ioannidou et al. investigated the cause and consequences of adipocyte growth and obese state in a spheroid culture method by providing a natural growth niche composed of vascular endothelial sprouts and ECM for the differentiation of preadipocytes into unilocular human adipocytes, which they termed HUVAS (human unilocular vascularized adipocyte spheroids). They also added immune cells and all the cells were embedded in growth factor-reduced (GFR) Matrigel™ (Fig. 3d-f). Spheroid structures were obtained by seeding 10,000 cells per well in an ultra-low attachment 96-well plate with round bottom and grown without Matrigel™, or embedded in 40 µL GFR Matrigel™ at day 6, then cultured for up to 40 days. Lipid treated HUVAS adipocytes accompanied many of the key features of adipocyte dysfunction, including a lower adiponectin-leptin secretion ratio, increased cytokine secretion, decreased insulin response, and dysfunctional lipolysis than non-treated control groups. In addition, Matrigel™-embedded spheroids displayed improved adipocyte morphology and larger lipid droplets with unilocular cells [175].

3.2. Brown adipose tissue reconstruction

Brown adipose tissue (BAT) is characterized by specialized cells containing a large number of mitochondria and plays an active role in energy metabolism. Therefore, the generation of 3D *in vitro* BAT has production potential for the treatment and investigation of obesity and T2DM associated with disturbances in the energy balance of the body. Another main characteristic of BAT is that it has a highly organized vasculature system [176]. For this reason, it is extremely important to ensure a successful vascular network to preserve the metabolic functions of the implanted BAT structure. Moreover, every brown adipocyte is surrounded by a thick basal membrane (BM) containing collagen IV as a major component and laminin as the most abundant non-collagenous protein and also fibronectin-1 [177–179]. Therefore, the use of these and similar polymers in tissue engineering studies for BAT might be a promising approach in terms of mimicking the native tissue.

Scientific publications on AT have mostly focused on WAT engineering, while studies on BAT engineering have been recent and are relatively scarce. Generally, the cells used in these studies are stem cells derived from human, rat or mouse AT, while the matrices used as scaffolds have varied. In the studies examined, synthetic polymers (e.g., PEG and its derivatives [24,179]) and natural polymers, such as collagen [62] or HA [49] were used with or without chemical modification as the hydrogel matrix for *in vitro* BAT fabrication. Apart from these, there is also a study with commercially available materials were used, such as HistoGel™ [180]. Table 2 lists the materials used for BAT reconstruction.

In a recent study, the vascularization capacity of WAT and BAT grafts were compared. Isolated size-matched grafts from the inguinal WAT pad and interscapular BAT depot of C57BL/6N mice were transplanted on recipient mice and observed for 14 days. According to the results, while WAT grafts demonstrated functional microvessel density and architecture as in native WAT, the BAT grafts had an erratic vascular structure and lower functional microvessel density when compared with native BAT. Although both tissue types were well vascularized, the BAT grafts could not be successfully and fully grafted onto the host due to their high metabolic demands [181]. These results emphasize the need for vascularized BAT substitutes and the challenges of implantation of BAT grafts.

To recreate vascularized BAT *in situ*, Tharp et al. subcutaneously implanted acrylated HA hydrogels modified with reactive bioactive peptides (CGGKAFDITYVRLKF and CGGRKRLQVQLSIRT) and mouse-derived WAT-derived ADSCs to recipient mice. Accordingly, the 3D engineered structures were highly vascularized at a macroscopic level by attracting the vasculature of the host recipient and were able to maintain UCP1 expression for several weeks. They also showed that modification with peptides actually increased the expression of UCP1 in 2D culture on tissue culture polystyrene plates coated with the bioactive peptides [49].

There is some evidence that angiogenic factors such as VEGF and FGF2 (fibroblast growth factor 2) modulate brown adipogenic potential [182,183]. For this purpose, Kuss et al. evaluated the effects of the endothelial growth environment on the brown adipogenic precursor cells, demonstrating that angiogenic factors increase brown adipogenic potential through epigenetic mechanisms by observing results such as increased expression of UCP1 and a decrease in histone deacetylase 1 (HDAC1) which is the negative regulator of brown adipocyte thermogenic production[183].

Matrix stiffness and porosity can be important factors in the differentiation of white or brown adipocytes. Accordingly, in the same study, the effects of methacrylated HA and methacrylated gelatin based soft (2.02 ± 1.11 kPa), (9.17 ± 3.14 kPa) and stiff porous (9.00 ± 2.38 kPa) hydrogels on adipocyte differentiation were investigated. It was concluded that while soft hydrogels support white adipogenic cell differentiation, stiff-porous hydrogels are optimal for BAT adipogenesis [183].

In another report, Hafner et al. showed that human induced pluripotent stem cells (iPSC) exposed to endothelial growth medium acquire a multilocular structure and differentiate into brown-like adipose progenitors [184].

Hammel et al. carried out a 3D-cell culture study by co-culturing adipocytes and HUVECs in collagen type 1 hydrogels to create a vascular formation. Firstly, MSCs were pre-differentiated to adipocytes *in vitro* and the differentiated adipocytes were then co-cultured with ECs. I t was observed how both the presence and density of ECs affects adipocyte development and organization and they established a link between vascular density and adipocyte maturation with this 3D *in vitro* model. It was observed that the 1:1 co-culture condition resulted in significantly higher vessel diameters and branches, and the authors concluded that this condition resulted in optimal vascular network formation with VEGF supplementation. This study also showed that the presence of ECs is effective in the browning of adipocytes via PGC1α [62].

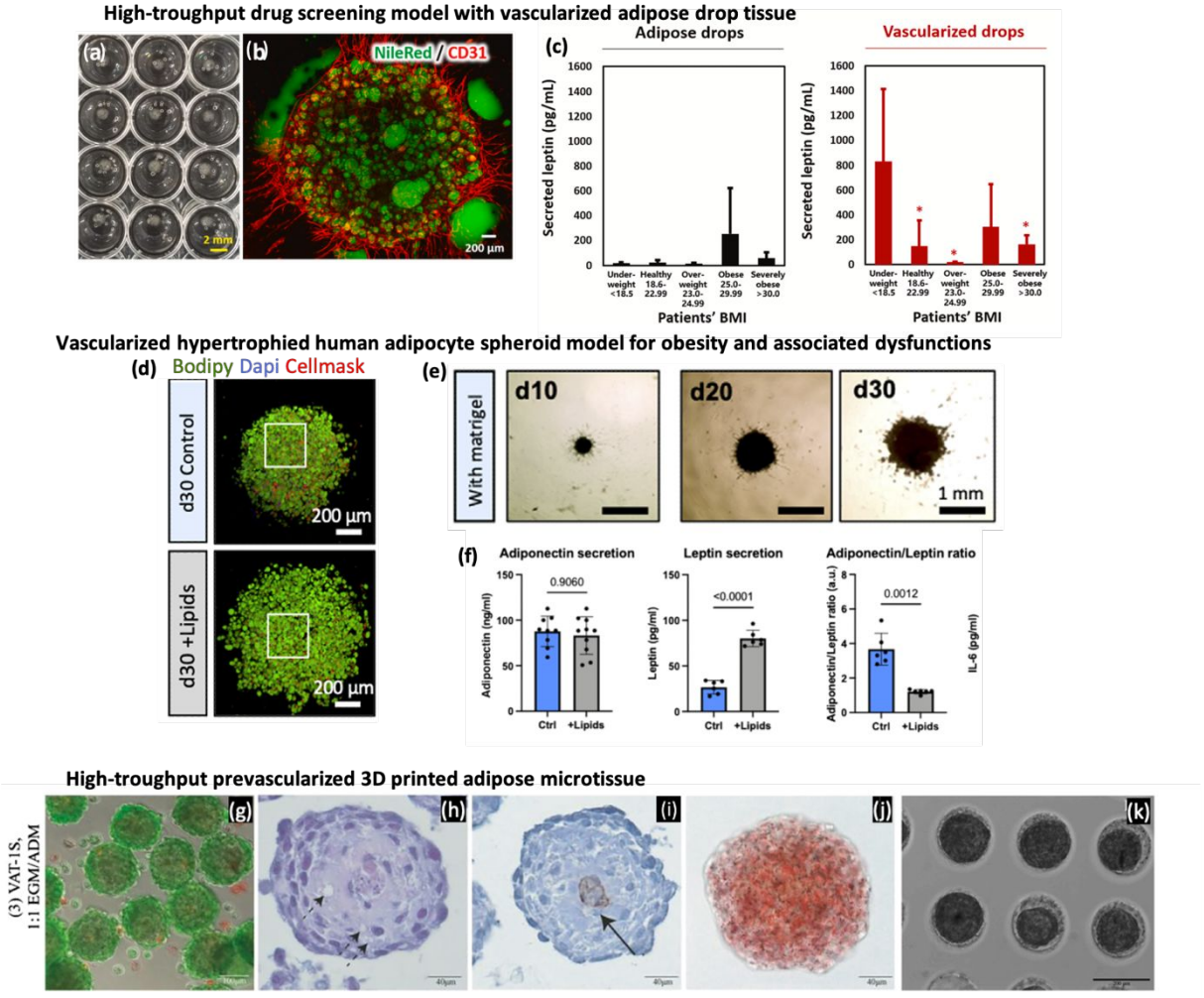

Fig. 3. Drug screening models against obesity and diabetes. (a-c) Vascularized adipose drop model for high-throughput drug screening. (a) Vascularized adipose drops in a 96-well plate after gelation. (b) Representative Nile Red (lipids) and CD31 (blood vessels) projection staining images after 1 week of culture in the vascularized adipose drop model. (c) Leptin secretion profiles according to the BMI ranges of the patients whose adipose tissues were isolated. Significant differences were compared to the underweight range. The graphs show results as means ± SD of experiments performed on n = 6-8 drops per condition per donor (This content is shown under the Creative Commons Attribution 4.0 International License (CC-BY-NC-ND 4.0); adapted from reference 65). (d-f) Vascularized hypertrophied human adipocyte spheroids as obesity and associated dysfunctions. (d) Representative fluorescent microscopy images of adipocyte spheroids cultured on day 30 (d30) without or with lipids, and stained with BODIPY (green), DAPI (blue) and lectin (red), showing lipid-treated spheroids containing larger lipid droplets. (e) Constructing vasculature-guided adipocyte spheroids by embedding in Matrigel™ on day 10 (d10), day 20 (d20) and day 30 (d30). (f) Control and lipid-treated spheroid secretion of adiponectin and leptin to the cell culture media on d30, as well as the ratio of the two. Each dot represents one spheroid, n = 10 spheroids per condition for adiponectin and 6 spheroids per condition for leptin and the adiponectin/leptin ratio. Data are presented as means ± SD and statistics were calculated using Student's unpaired t-test (This content is shown under the Creative Commons Attribution 4.0 International License (CC-BY-NC-ND 4.0); adapted from reference 175). (g-k) High-throughput prevascularized 3D printed adipose microtissue. (g-j) VAT-1S ASC/HUVEC spheroids, day 14. Premixed ASC/HUVEC spheroids (262 cells per spheroid) were co-cultured for 14 days in 1:1 EGM(endothelial growth medium)/ADM (adipogenic differentiation medium). Analyses for Ca/PI (g), HE, (h) CD31 IHC (i), Oil Red O (j) were performed after 14 days of co-culture. Black and dotted arrow represents capillary-like structures and lipid droplets, respectively. Scale bar = 40 µm. (k) Phase contrast microscopy of the spheroids on day 14. VAT-1S ASC/HUVEC spheroids in 1:1 EGM/ADM (262 cells per spheroid), which can be held representative for the two other co-culture conditions 1:1 EGM/ADM. Scale bar = 200 µm. VAT-1S: Vascularized adipose tissue-one step. Reproduced with permission from reference 192. Copyright 2020, John Wiley and Sons.

This journal is © The Royal Society of Chemistry 20xx

From this point of view, it can be concluded that to obtain engineered, highly-vascularized BAT, including conditions such as an endothelial growth environment that promotes capillary structure, and cells that can promote vascularization such as ECs, smooth muscle cells and pericytes might give successful results.

MVFs which are microvessel units that can be isolated from large adipose tissues by enzymatic digestion [185], can be an effective method for obtaining vascularized thermogenic AT, as they can rapidly reassemble new microvascular pathways in the host tissue after implantation. 'This is because MVFs, including small arterioles, venules and capillaries, are rich in macrophages, T-cells, progenitor cells (white and brown precursors), perivascular stem cells with multidifferentiation potential, myeloid cells, hematopoietic cells, pericytes and ECs? [47,48,186]. In a recent study, functional beige AT microtissues were developed by suspending MVFs isolated from human subcutaneous AT in fibrin gel. While the structures cultured in white, beige adipogenic differentiation and growth medium for 14 days showed similar results in terms of vascularization (percentage of well coverage around 0.3 to 0.5%), the structures cultured in beige medium exhibited increased glucose uptake, higher expression of brown related markers (such as UCP1), and gave better results in terms of improved cellular respiration compared to the other groups [48].

In another related report, vascularized beige AT structures were obtained *in vitro* with MVFs isolated from lean and diabetic rat models and examined in terms of beige and vascularization characteristics. After 14 days of *in vitro* cultivation, the structures taken from the lean rat caused higher angiogenesis with an interconnected network compared to the MVF group of diabetic origin, regardless of the culture medium. In addition, lipid droplets accumulations of lipid droplets with branched vessel formation were observed in groups cultured in white and beige differentiation media. However, the effect of the difference between diabetic and lean MVFs on the obtained beige characteristics is yet to be ascertained [186].

In a study investigating whether MVFs are a source of thermogenic adipose tissue, beige adipose microtissues were developed using human MVFs isolated from a patient over 50 years of age, and autologous sources from adult patients were evaluated (Fig. 2g-k). The MVFs were cultivated in growth, white, and beige adipogenic media (Fig. 2g-i). While a vascular structure was observed in all groups, a higher oxygen consumption rate was recorded in the groups incubated in beige adipogenic (BAM) and white adipogenic differentiation medium (WAM) compared to the growth medium (GM) group (16.63 ± 8.1 pmol/min, 15.1 ± 9.2 pmol/min, and 7.2 ± 4.1 pmol/min respectively) (Fig. 2j). In addition, according to GS lectin staining for vascular structure visualization, the BAM group showed a relatively higher result in terms of lectin well coverage percentage with around 0.5% while GM and WAM groups were around 0.3% to 0.4% (Fig. 2k) [187].

Table 2. Materials used for BAT reconstruction

Material	**Cell Used**	**Prevascularization *in vitro***	**Neovascularization *in vivo***	**Remarks**	**References**
Collagen type I	Human MSC and HUVEC	Yes	No	*In vitro* vasculogenesis and brown adipogenesis	62
Acrylated hyaluronic acid	Mouse ADSC	No	Yes	Vasculogenesis and brown adipogenesis occurred after *in vivo* implantation	49
Methacrylated hyaluronic and methacrylated gelatin	Human white- and brown-adipose stromal vascular cells	No	No	*In vitro* white and brown adipogenesis	183
Histogel™	Human ADSC and HUVEC	Yes	No	*In vitro* angiogenesis and brown adipogenesis	180
PEGDA	Mouse ADSC	No	No	*In vitro* brown adipogenesis	179
	Human and rat White and brown ADSC	No	No	*In vitro* brown and white adipogenesis	24

3.3. Breast reconstruction

Breast cancer is the world's most prevalent type of cancer with 2.3 million women worldwide diagnosed in 2020 and 685,000 deaths in the same year according to WHO data [188]. For this reason, remodelling and reconstruction of the breast after mastectomy for cancer is of great importance. Breast reconstruction is a challenging area of tissue engineering that requires the regular organization of many different cell types and a strong vascular network in a high-scale size tissue. To date, researchers have worked in the field of biomaterials, regenerative medicine and plastic surgery and carried out various studies by focusing on many factors such as appropriate shape, volume and mechanical properties to realize effective breast reconstruction for patients. In addition to the purpose of restructuring the breast after cancer, reconstruction can also be performed for cosmetic reasons. Most of these treatments are implant-based (69%), while the rest are autologous flap reconstruction (31%) [189]. Moreover, the reabsorption rate for autologous fat grafts, which is a well-known technique, is 40-60% of the injected volume mostly due to the lack of revascularization after injection [13]. Regardless of the reason for the need for breast reconstruction, the key issues in the intervention are aesthetic quality, patient satisfaction, and low complication rate [190]. The biomaterial used for this purpose should have properties such as appropriate biodegradation, biocompatibility, non-toxicity, have compatibility with blood, and be both non-inflammatory and non-allergic. In this way, the natural structure of the breast can be achieved, augmented or remodelled [189]. As clinical application necessitates a move to higher scale tissues, bioprinting has recently been proposed as an appropriate technique for this purpose. For these applications, prevascularization before implantation appears to be of even greater importance. An example is the direct bioprinting of mature adipocytes to ensure a final mature tissue, using a collagen microfiber-containing bioink in a gellan gum support bath which can achieve a fully vascularized AT [143]. Then, for *in vivo* validation, bigger animals are first used for the pre-clinical assessment. In this context, Chhaya et al. implanted scaffolds made of PCL which were similar to silicone implant geometry into the subglandular pockets of immunocompromised minipigs for 24 weeks. According to the results of the research, which was carried out with 3 experimental groups: empty scaffolds, scaffolds containing 4 cm^3 lipoaspirate, and a lipoaspirate injected group after 2 weeks of prevascularization, angiogenesis and AT formation were observed in all groups. It was also reported that the prevascularization group was superior in terms of vascularization and AT formation [191].

Benmaridje et al. developed prevascularized spheroids obtained by ASC and HUVEC co-culture and bioprinted them with GelMA hydrogel in a high-throughput manner for potential applications such as *in vitro* drug screening and an angiogenesis model (Fig. 3g-k). The microtissues showed high adipogenic differentiation and capillary-like formation at days 7 and 14 [192]. This strategy might be a promising approach to perform drug tests on vascularized AT or to simulate the conditions with low vascularization such as obesity.

4. Conclusion and potential applications

AT engineering is an interesting field that has been studied across a wide range of clinical and medical applications such as drug screening, 3D modelling of AT-based organs and related-diseases, plastic and reconstructive surgery. The main challenge of AT engineering is to reproduce the complex 3D structure of each component *in vitro* starting from the polymeric content of tissue ECM with sufficient vascularization. In particular, the use of materials which stimulate the vascularization nature of the tissue is advantageous in terms of alternatives or supplements to existing clinical options. It is necessary to establish an effective blood supply to limit damage from hypoxic conditions in a tissue volume which can be used clinically. Accordingly, the combination of engineered AT materials with vascularization strategies is an important matter that needs to be addressed.

Both *in vitro* and *in vivo* AT tissue engineered substitutes must provide long-term stability to be incorporated into the host vasculature and maintain their structural organization. This can be made possible with the formation of an adequate vascular network to ensure and maintain stability. The vascular structure is important for the adequate delivery of nutrients and oxygen into the tissue, thus maintaining the structural organization. Therefore, the blood vessel structure must be added *in vitro* or created *in situ* by *de novo* angiogenesis [1].

Strategies for AT engineering; innovative approaches such as injectable scaffold materials and 3D bioprinting technologies are promising approaches, especially 3D models which provide neovascularization. In Fig. 4, some of the possibilities for the biofabrication of vascularized AT models are shown. For AT biofabrication, which has a very common application area, not only materials that function as fillers, but also injectable materials that support adipogenesis and even angiogenesis are needed. Therefore, the use of injectable hydrogels is an important strategy as they are a minimally invasive technique among scaffold-based methods for AT regeneration [13]. Compared to porous tissue scaffolds, it is also advantageous in removing irregular tissue defects due to its pre-gelling properties with minimal invasiveness [193]. Also, Torio-Padron et al. showed that neovascularization was induced by injecting different cell concentrations of human preadipocytes with fibrin matrices into athymic nude mice [98]. Cho et al. performed the injection of human preadipocytes suspended in fibrin under a dome-shaped support structure obtained from poly(glycolic acid) (PGA) fiber-based matrices reinforced with poly(l-lactic acid) (PLLA) implanted subcutaneously in athymic mice to produce a volume-stable AT formation which was observed at the implantation site after 6 weeks [194]. Kawaguchi et al. reported that by subcutaneously injecting bFGF (basic fibroblast growth factor) loaded Matrigel™ with 3T3-F442A preadipocytes in mice, neovascularization occurred within 1 week [82]. As seen in these examples, and in addition to these, other studies [76,80,81,85,88,106] in which active vascularization occurs

This journal is © The Royal Society of Chemistry 20xx

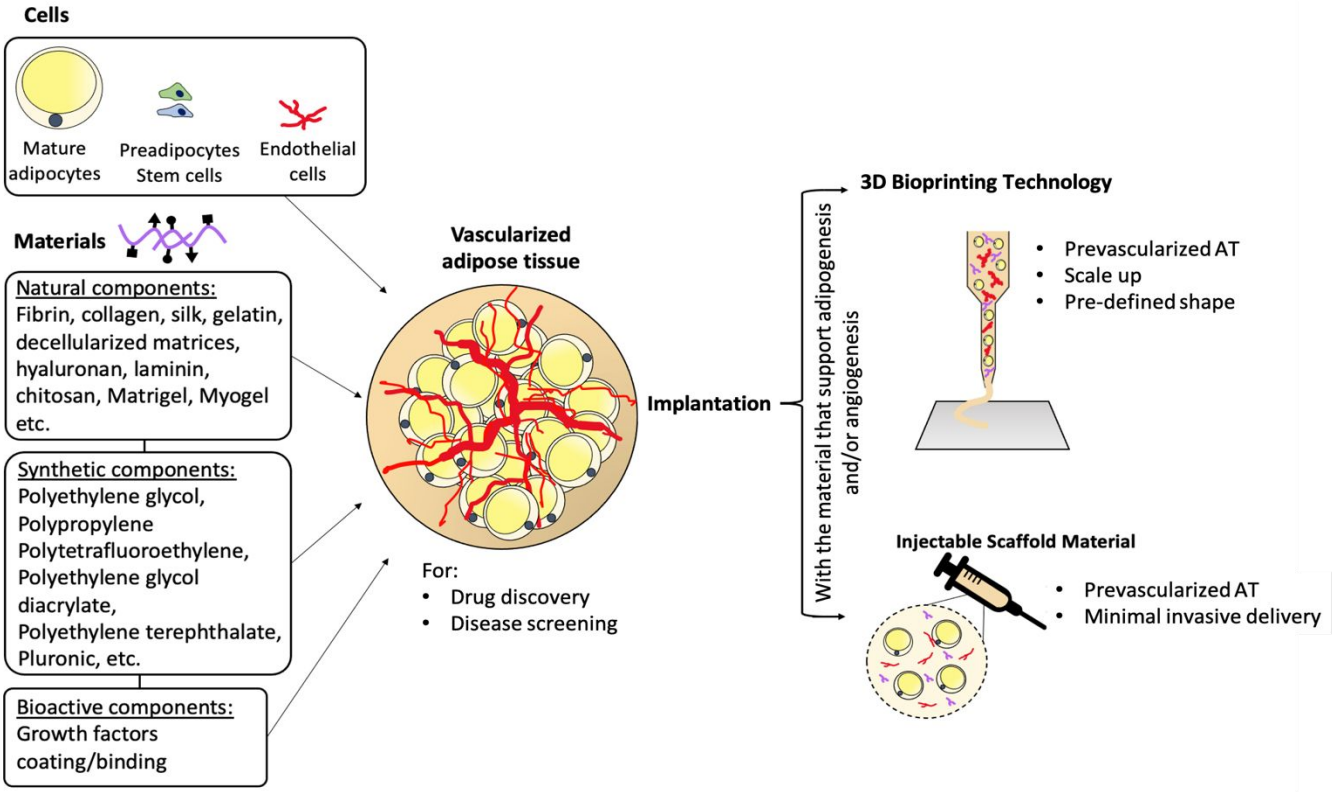

Fig. 4. Perspective possibilities for a perfect model for vascularized AT. Cells and vascular structure are significant components for vascularized and functional adipose tissue biofabrication. Implantation with a material that supports adipogenesis and/or angiogenesis might be a possible application method for predefined shape and prevascularized constructs by minimal invasiveness. The obtained models can be used for drug discovery and disease screening.

after *in vivo* injection also highlight the importance of AT engineering applications with injectable materials. Besides the applications of injectable polymers in AT engineering, another innovative AT modelling approach to obtain vascularized substitutes is 3D bioprinting. Bioprinting enables the reproducible production of complex living tissues, while reproducing native tissue-specific vascular complexity [195,196]. This makes 3D bioprinting technology popular for the production of AT models. Saljö et al. injected human AT-derived lipoaspirate into nude mice by 3D bioprinting with an alginate/nanocellulose bioink and reported that, after 30 days, new blood vessels had formed on the surface of the grafts [196]. Huber et al. observed high cell viability and adipogenic gene expressions during a 14-day culture period by encapsulating mature human adipocyte spheroids in photo-crosslinked GelMA hydrogels [148]. Louis et al. bioprinted mature adipocytes by encapsulating physiological collagen microfibers in a gellan gum-supported bath, and the resulting multilayer structures remained highly viable even after 7 days of culture [143].

Consequently, substitutions that recapitulate the functions and development of vascularized AT engineering will provide inspiration for future in vitro and *in vivo* studies and facilitate systematic evaluation of AT types. Even though many synthetically and naturally derived polymers have long been used for adipose tissue engineering purposes, naturally derived compounds such as fibrin and collagen are the most advantageous thanks to their adipogenesis and angiogenesis supporting characteristics. As 3D AT models become more accessible at a reproducible level, it is expected that implantable AT products will become widespread and drug discovery or screening studies for obesity, diabetes and metabolic diseases will be accelerated by shortening preclinical evaluation processes and increasing prediction accuracy.

Author Contributions

Aslı Sena Karanfil contributed to writing the original draft, visualization, conceptualization and investigation. Fiona Louis contributed to writing review and editing, supervision, validation and methodology. Michiya Matsusaki contributed to writing review, editing and supervision.

Conflicts of interest

There are no conflicts to declare.

Acknowledgements

This work was supported by a Grant-in-Aid for Scientific Research (A) (20H00665), Mirai-Program (18077228) from JST, and a project (JPNP20004) subsidized by the New Energy and Industrial Technology Development Organization (NEDO). The author acknowledges financial support from the Japanese Government (Monbukagakusho: MEXT) Scholarship.

References

1. F. Louis and M. Matsusaki, *Adipose tissue engineering*, Biomaterials for Organ and Tissue Regeneration, 2020, 393-423. DOI: https://doi.org/10.1016/B978-0-08-102906-0.00008-8.
2. S. Niemala, S. Miettinen, J. R. Sarkanen and N. Ashammakhi, *Topics in Tissue Engineering*, 2008, **4**, 1–26.
3. E. C. M. Mariman and P. Wang, *Cell Mol Life Sci*, 2010, **63**, 1277–1292. DOI: 10.1007/s00018-010-0263-4.
4. E. D. Rosen and O. A. MacDougald, *Nat Rev Mol Cell Biol*, 2006, **7**, 885–896. DOI: 10.1038/nrm2066.
5. A. G. Cristancho and M. A. Lazar, *Nat Rev Mol Cell Biol*, 2011, **12**, 722–734. DOI: 10.1038/nrm3198.
6. L. Z. Sharp, K. Shinoda, H. Ohno, D. W. Scheel, E. Tomoda, L. Ruiz, H. Hu, L. Wang, Z. Pavlova, V. Gilsanz and S. Kajimura, *PLoS One*, 2012, **7**, e49452. DOI: 10.1371/journal.pone.0049452.
7. M. Esteve Ràfols, *Endocrinol Nutr (English Ed)*, 2014, **61**, 100–112. DOI:10.1016/j.endoen.2014.02.001.
8. K. Aubin, M. Safoine, M. Proulx, M. A. Audet-Casgrain, J. F. Côté, F. A. Têtu, A. Roy and J. Fradette, *PLoS One*, 2015, **10**, 1–24. DOI: https://doi.org/10.1371/journal.pone.0137612.
9. S. Cinti, *Nutr Metab and Cardiovasc Dis*, 2006, **16**, 569–574. DOI: 10.1016/j.numecd.2006.07.009.
10. B. Cannon and J. Nedergaard, *Physiol Rev*, 2004, **84**, 277–359. DOI: 10.1152/physrev.00015.2003.
11. A. M. Cypess, S. Lehman, G. Williams, I. Tal, D. Rodman, A. B. Goldfine, F. C. Kuo, E. L. Palmer, Y. H. Tseng, A. Doria, G. M. Kolodny and C. Ronald Kahn*, Obstet Gynecol Surv*, 2009, **64**, 519–520. DOI: 10.1056/NEJMoa0810780.
12. J. H. Choi, J. M. Gimble, K. Lee, K. G. Marra, J. P. Rubin, J. J. Yoo, G. Vunjak-Novakovic and D. L. Kaplan, *Tissue Eng Part B Rev*, 2010, **16**, 413–426. DOI: 10.1089/ten.teb.2009.0544.
13. C. Conci, L. Bennati, C. Bregoli, F. Buccino, F. Danielli, M. Gallan, E. Gjini and M. T. Raimondi, *J Tissue Eng Regen Med*, 2020, **14**, 369–387. DOI: 10.1002/term.2999.
14. P. Kamat, F. S. Frueh, M. McLuckie, N. Sanchez-Macedo, P. Wolint, N. Lindenblatt, J. A. Plock, M. Calcagni and J. Buschmann, *Cytotherapy*, 2020, **22**, 400–411. DOI: https://doi.org/10.1016/j.jcyt.2020.03.433.
15. E. Donnely, M. Griffin and P. E. Butler, *Ann Biomed Eng*, 2020, **48**, 9–25. DOI: 10.1007/s10439-019-02373-3.
16. A. Sterodimas, J. de Faria, B. Nicaretta and I. Pitanguy, *J Plast Reconstr Aesthet Surg*, 2010, **63**, 1886–1892. DOI: 10.1016/j.bjps.2009.10.028.
17. A. C. Volz, L. Hack, F. B. Atzinger and P. J. Kluger, *ALTEX*, 2018, **35**, 464-476. DOI: 10.14573/altex.1802191.
18. G. Yang, B. Mahadik, J. Y. Choi and J. P. Fisher, *Prog Biomed Eng*, 2020, **2**, 012002. DOI: 10.1088/2516-1091/ab5637.
19. A. C. Volz, B. Huber and P. J. Kluger, *Differentiation*, 2016, **92**, 1-2. DOI: 10.1016/j.diff.2016.02.003.
20. R. Gianni-Barrera, N. di Maggio, L. Melly, M. G. Burger, E. Mujagic, L. Gürke, D. J. Schaefer and A. Banfi, *Stem Cells Transl Med*, **9,** 433-444. DOI: 10.1002/sctm.19-0319.
21. T. Osaki, V. Sivathanu and R. D. Kamm, *Curr Opin Biotechnol*, 2018, **52,** 116-123. DOI: 10.1016/j.copbio.2018.03.011.
22. M. V. Plikus, C. F. Guerrero-Juarez, M. Ito, Y. R. Li, P. H. Dedhia, Y. Zheng, M. Shao, D. L. Gay, R. Ramos, T. C. Hsi, J. W. Oh, X. Wang, A. Ramirez, S. E. Konopelski, A. Elzein, A. Wang, R. J. Supapannachart, H. L. Lee, C. H. Lim, A. Nace, A. Guo, E. Treffeisen, T. Andl, R. N. Ramirez, R. Murad, S. Offermanns, D. Metzger, P. Chambon, A. D. Widgerow, T. L. Tuan, A. Mortazavi, R. K. Gupta, B. A. Hamilton, S. E. Millar, P. Seale, W. S. Pear, M. A. Lazar and G. Cotsarelis, *Science (1979)*, 2017, **355**, 748–752. DOI: 10.1126/science.aai8792.
23. A. M. Unser, B. Mooney, D. T. Corr, Y. H. Tseng and Y. Xie, *Biomaterials*, 2016, **75**, 123–134. DOI: 10.1016/j.biomaterials.2015.10.017.
24. J. P. Yang, A. E. Anderson, A. McCartney, X. Ory, G. Ma, E. Pappalardo, J. Bader and J. H. Elisseeff, *Tissue Eng Part A*, 2017, **23**, 253–262. DOI: 10.1089/ten.TEA.2016.0399.
25. K. Bódis and M. Roden, *Eur J Clin Invest*, 2018, **48**, e13017. DOI: 10.1111/eci.13017.
26. N. Shoham and A. Gefen, *J Biomech*, 2012, **45**, 1–8. DOI: https://doi.org/10.1016/j.jbiomech.2011.10.023
27. B. D. Pope, C. R. Warren, K. K. Parker and C. A. Cowan, *Trends Cell Biol*, 2016, **26**, 745–755. DOI: 10.1016/j.tcb.2016.05.005.
28. N. Alkhouli, J. Mansfield, E. Green, J. Bel, B. Knight, N. Liversedge, J. C. Tham, R. Welbourn, A. C. Shore, K. Kos and C. P. Winlove, *Am J Physiol Endocrinol Metab*, 2013, **305**, 1427–1435. DOI: 10.1152/ajpendo.00111.2013
29. J. H. Stern and P. E. Scherer, *Nat Rev Endocrinol*, 2015, **11**, 71–72. DOI: 10.1038/nrendo.2014.219.
30. D. Tupone, C. J. Madden and S. F. Morrison, *Front Neurosci*, 2014, **8**, 1–14. DOI: 10.3389/fnins.2014.00014
31. N. H. Rogers, *Ann Med*, 2015, **47**, 142–149. DOI: 10.3109/07853890.2014.914807.
32. V. Lecoultre and E. Ravussin, *Curr Opin Clin Nutr Metab Care*, 2011, **14**, 1–6. DOI: 10.1097/MCO.0b013e328341221e.
33. K. Townsend and Y.-H. Tseng, *Adipocyte*, 2012, **1**, 13–24. DOI: 10.4161/adip.18951.
34. A. M. Bertholet and Y. Kirichok, *Biochimie*, 2017, **134**, 28–34. DOI: 10.1016/j.biochi.2016.10.013.
35. J. Nedergaard and B. Cannon, *Biochim Biophys Acta Mol Cell Biol Lipids*, 2013, **1831**, 943–949. DOI: 10.1016/j.bbalip.2013.01.009.
36. W. D. van Marken Lichtenbelt, J. W. Vanhommerig, N. M. Smulders, J. M. A. F. L. Drossaerts, G. J. Kemerink, N. D.

This journal is © The Royal Society of Chemistry 20xx

Bouvy, P. Schrauwen and G. J. J. Teule, *New England Journal of Medicine*, 2009, **360**, 1500–1508. DOI: 10.1056/NEJMoa0808718.
37. K. Shinoda, I. H. N. Luijten, Y. Hasegawa, H. Hong, S. B. Sonne, M. Kim, R. Xue, M. Chondronikola, A. M. Cypess, Y. H. Tseng, J. Nedergaard, L. S. Sidossis and S. Kajimura, *Nat Med*, 2015, **21**, 389–394. DOI: 10.1038/nm.3819.
38. A. M. Cypess, A. P. White, C. Vernochet, T. J. Schulz, R. Xue, C. A. Sass, T. L. Huang, C. Roberts-Toler, L. S. Weiner, C. Sze, A. T. Chacko, L. N. Deschamps, L. M. Herder, N. Truchan, A. L. Glasgow, A. R. Holman, A. Gavrila, P. O. Hasselgren, M. A. Mori, M. Molla and Y. H. Tseng, *Nat Med*, 2013, **19**, 635–639. DOI: 10.1056/NEJMoa0810780.
39. J. M. Weitzel, K. A. H. Iwen and H. J. Seitz, *Exp Physiol, 2003,* **88***,* 121–128*.* DOI: 10.1113/eph8802506.
40. F. Seebacher and E. J. Glanville, *PLoS One*, 2010, **5**, 1–8. DOI: https://doi.org/10.1371/journal.pone.0013022.
41. S. Lim, J. Honek, Y. Xue, T. Seki, Z. Cao, P. Andersson, X. Yang, K. Hosaka and Y. Cao, *Nat Protoc*, 2012, **7**, 606–615. DOI: 10.1038/nprot.2012.013
42. A. Krings, S. Rahman, S. Huang, Y. Lu, P. J. Czernik and B. Lecka-Czernik, *Bone*, 2012, **50**, 546–552. DOI: 10.1016/j.bone.2011.06.016
43. K. Xu, R. Xie, X. Lin, J. Jia, N. Zeng, W. Li, D. Xiao and T. Du, *Transplantation*, 2020, **104**, 2059–2064. DOI: 10.1097/TP.0000000000003322.
44. A. Kuryłowicz and M. Puzianowska-Ku´znickaku´znicka, *Int J Mol Sci,* **21**, 6241. DOI:10.3390/ijms21176241.
45. M. Giralt and F. Villarroya, *Endocrinology*, 2013, **154**, 2992–3000. DOI: 10.1210/en.2013-1403.
46. T. C. L. Bargut, V. Souza-Mello, M. B. Aguila and C. A. Mandarim-De-Lacerda, *Horm Mol Biol Clin Investig*, 2017, **31**, 1–13. DOI: 10.1515/hmbci-2016-0051.
47. F. M. Acosta, K. Stojkova, E. M. Brey and C. R. Rathbone, *Tissue Eng Part A*, 2020, **26**, 905–914. DOI: 10.1089/ten.TEA.2019.0345.
48. M. A. Gonzalez Porras, K. Stojkova, F. M. Acosta, C. R. Rathbone and E. M. Brey, *Front Bioeng Biotechnol*, 2022, **10**. DOI: 10.3389/fbioe.2022.906395.
49. K. M. Tharp, A. K. Jha, J. Kraiczy, A. Yesian, G. Karateev, R. Sinisi, E. A. Dubikovskaya, K. E. Healy and A. Stahl, *Diabetes*, 2015, **64**, 3713–3724. DOI: 10.2337/db15-0728.
50. J. Diedrich, H. C. Gusky and I. Podgorski, *Horm Mol Biol Clin Investig*, **21**, 17-41. DOI: 10.1515/hmbci-2014-0045.
51. K. J. Suchacki, W. P. Cawthorn and C. J. Rosen, *Curr Opin Pharmacol*, 2016, **28**, 50-56. DOI: 10.1016/j.coph.2016.03.001.
52. M. J. Devlin, A. M. Cloutier, N. A. Thomas, D. A. Panus, S. Lotinun, I. Pinz, R. Baron, C. J. Rosen and M. L. Bouxsein, *J of Bone Miner Res*, 2010, **25**, 2078-2088. DOI: 10.1002/jbmr.82.
53. H. Fairfield, C. Falank, M. Farrell, C. Vary, J. M. Boucher, H. Driscoll, L. Liaw, C. J. Rosen and M. R. Reagan, *Bone*, 2019, **118**, 77–88. DOI: 10.1016/j.bone.2018.01.023.
54. A. Ravichandran, C. Meinert, O. Bas, D. W. Hutmacher and N. Bock, *Mater Sci Eng C*, 2021, **128**, 112313. DOI: 10.1016/j.msec.2021.112313.
55. S. Cinti, *Trends Endocrinol Metab*, 2018, **29**, 651–666. DOI: https://doi.org/10.1016/j.tem.2018.05.007
56. A. Giordano, A. Smorlesi, A. Frontini, G. Barbatelli and S. Cint, *Eur J Endocrinol*, 2014, **170,** R159-71. DOI: 10.1530/EJE-13-0945.
57. M. Yilmaz and G. S. Hotamisligil, *Cell Metab*, 2013, **17**, 7–9. DOI: http://dx.doi.org/10.1016/j.cmet.2012.12.014
58. J. G. Neels, T. Thinnes and D. J. Loskutoff, *The FASEB Journal*, 2004, **18**, 983-985, DOI: 10.1096/fj.03-1101fje.
59. B. Vailhé, D. Vittet and J. J. Feige, *Lab Investig*, 2001, **81**, 439-452. DOI: 10.1038/labinvest.3780252.
60. K. Sun, C. M. Kusminski, P. E. Scherer, *J Clin Invest*, 2011, **121**, 2094–2101. DOI: 10.1172/JCI45887.
61. S. Corvera and O. Gealekman, *Biochim Biophys Acta - Mol. Basis Dis*, 2014, **1842**, 463-472. DOI: 10.1016/j.bbadis.2013.06.003.
62. J. H. Hammel and E. Bellas, *Integr Biol (Camb)*, 2020, **12**, 81–89. DOI: 10.1093/intbio/zyaa006.
63. K. Sun, C. M. Kusminski, K. Luby-Phelps, S. B. Spurgin, Y. A. An, Q. A. Wang, W. L. Holland and P. E. Scherer, *Mol Metab*, 2014, **3**, 474–483. DOI: 10.1016/j.molmet.2014.03.010
64. S. Aoki, S. Toda, T. Sakemi and H. Sugihara, *Cell Struct Funct*, 2003, **28**, 55–60. DOI: 10.1247/csf.28.55.
65. F. Louis, Y. Sowa, S. Kitano and M. Matsusaki, *Bioact Mater*, 2022, **7**, 227–241. DOI: https://doi.org/10.1016/j.bioactmat.2021.05.020.
66. J. Borges, M. C. Müller, A. Momeni, G. B. Stark and N. Torio-Padron, *Minim Invasive Ther Allied Technol*, 2007, **16**, 141–148. DOI: 10.1080/13645700600935398.
67. N. Lai, A. Jayaraman and K. Lee, *Tissue Eng Part A*, **15**, 1053-1061. DOI: 10.1089/ten.tea.2008.0101.
68. J. H. Kang, J. M. Gimble and D. L. Kaplan, *Tissue Eng Part A*, 2009, **15**, 2227–2236. DOI: 10.1089=ten.tea.2008.0469.
69. J. H. Choi, E. Bellas, G. Vunjak-Novakovic and D. L. Kaplan, *Methods Mol Biol*, 2011, **702**, 319–330. DOI: 10.1007/978-1-61737-960-4_23.
70. B. Huber, K. Borchers, G EM Tovar P. J. Kluger, *J Biomat Appl*, 2015, **30**, 699-710. DOI: 10.1177/0885328215587450
71. J. Ho, C. Walsh, D. Yue, A. Dardik and U. Cheema, *Adv Wound Care (New Rochelle)*, 2017, **6**, 191–209. DOI: 10.1089/wound.2016.0723.
72. C. W. Patrick, *Anatomical Record*, 2001, **263**, 361–366. DOI: 10.1002/ar.1113.
73. C. Brayfield, K. Marra and J. P. Rubin, *Handchir Mikrochir Plast Chir*, 2010, **42**, 124–128. DOI: 10.1055/s-0030-1248269.
74. I. van Nieuwenhove, L. Tytgat, M. Ryx, P. Blondeel, F. Stillaert, H. Thienpont, H. Ottevaere, P. Dubruel and S. van Vlierberghe, *Acta Biomater*, 2017, **63**, 37–49.

DOI: 10.1016/j.actbio.2017.09.026.

75. D. von Heimburg, S. Zachariah, H. Kühling, I. Heschel, H. Schoof, B. Hafemann and N. Pallua, *Biomaterials*, 2001, **22**, 429–438. DOI: 10.1016/s0142-9612(00)00186-1.
76. A. v. Vashi, K. M. Abberton, G. P. Thomas, W. A. Morrison, A. J. O'Connor, J. J. Cooper-White and E. W. Thompson, *Tissue Eng*, 2006, **12**, 3035–3043. DOI: 10.1089/ten.2006.12.3035.
77. C. H. Chuang, R. Z. Lin, J. M. Melero-Martin and Y. C. Chen, *Artif Cells Nanomed Biotechnol*, 2018, **46**, 434-447. DOI: 10.1080/21691401.2018.1499660.
78. Y. Kimura, M. Ozeki, T. Inamoto and Y. Tabata, *Biomaterials*, 2003, **24**, 2513–2521. DOI: 10.1016/s0142-9612(03)00049-8.
79. E. Bellas, K. G. Marra and D. L. Kaplan, *Tissue Eng Part C Methods*, 2013, **19**, 745–754. DOI: 10.1089/ten.TEC.2012.0620.
80. T. Schoeller, S. Lille, G. Wechselberger, A. Otto, A. Mowlawi and H. Piza-Katzer, *Aesthetic Plast Surg*, 2001, **25**, 57–63. DOI: 10.1007/s002660010096.
81. J. Borges, N. Torío-Padrón, A. Momeni, M. C. Mueller, F. T. Tegtmeier and B. G. Stark, *Minim Invasive Ther and Allied Technol*, 2014, **63**, 246–252. DOI: 10.1080/14017450600761620.
82. N. Kawaguchi, K. Toriyama, E. Nicodemou-Lena, K. Inou, S. Torii and Y. Kitagawa, *Proc Natl Acad Sci U S A*, 1998, **95**, 1062–1066. DOI: 10.1073/pnas.95.3.1062.
83. N. Kawaguchi, K. Toriyama, E. Nicodemou-Lena, K. Inou, S. Torii and Y. Kitagawa, *Cytotechnology*, 1999, **31**, 215–220. DOI: 10.1023/A:1008198731341.
84. F. Stillaert, M. Findlay, J. Palmer, R. Idrizi, S. Cheang, A. Messina, K. Abberton, W. Morrison and E. W. Thompson, *Tissue Eng*, 2007, **13**, 2291–2300. DOI: 10.1089/ten.2006.0382.
85. J. H. Piasecki, K. Moreno and K. A. Gutowski, *Aesthet Surg J*, 2008, **28**, 306–312. DOI: 10.1016/j.asj.2008.02.005.
86. K. Hemmrich, D. von Heimburg, R. Rendchen, C. di Bartolo, E. Milella and N. Pallua, *Biomaterials*, 2005, **26**, 7025–7037. DOI: 10.1016/j.biomaterials.2005.04.065.
87. L. Flynn, J. L. Semple and K. A. Woodhouse, *J Biomed Mater Res A*, 2006, **79**, 963–73. DOI: 10.1002/jbm.a.30762.
88. J. S. Choi, H. J. Yang, B. S. Kim, J. D. Kim, J. Y. Kim, B. Yoo, K. Park, H. Y. Lee and Y. W. Cho, *Journal of Controlled Release*, 2009, **139**, 2–7. DOI: 10.1016/j.jconrel.2009.05.034.
89. Y. C. Choi, J. S. Choi, B. S. Kim, J. D. Kim, H. I. Yoon and Y. W. Cho, *Tissue Eng Part C Methods*, 2012, **18**, 866–876. DOI: 10.1089/ten.tec.2012.0009.
90. C. Yu, J. Bianco, C. Brown, L. Fuetterer, J. F. Watkins, A. Samani and L. E. Flynn, *Biomaterials*, 2013, **34**, 3290–3302. DOI: 10.1016/j.biomaterials.2013.01.056.
91. T. T. Y. Han and L. E. Flynn, *J Tissue Eng Regen Med*, 2020, **14**, 1827–1840. DOI: 10.1002/term.3133.
92. K. Hemmrich and D. von Heimburg, *Expert Rev Med Devices*, 2006, **3**, 635–645. DOI: 10.1586/17434440.3.5.635.
93. S. Neuss, R. Stainforth, J. Salber, P. Schenck, M. Bovi, R. Knüchel and A. Perez-Bouza, *Cell Transplant*, 2008, **17**, 977–986. DOI: 10.3727/096368908786576462.
94. T. H. Chun, K. B. Hotary, F. Sabeh, A. R. Saltiel, E. D. Allen and S. J. Weiss, *Cell*, 2006, **125**, 577–591. DOI: 10.1016/j.cell.2006.02.050.
95. D. von Heimburg, M. Kuberka, R. Rendchen, K. Hemmrich, G. Rau and N. Pallua, *Int J Artif Organs*, 2003, **26**, 1064–1076. DOI: 10.1177/039139880302601204.
96. J. Takagi, *Biochem Soc Tran*, 2004, **32**, 403-406. DOI: 10.1042/BST0320403.
97. H. A. Strobel, T. Gerton and J. B. Hoying, *Biofabrication*, 2021, **13**, 035022. DOI: 10.1088/1758-5090/abe187.
98. N. Torio-Padron, N. Baerlecken, A. Momeni, G. B. Stark and J. Borges, *Aesthetic Plast Surg*, 2007, **31**, 285–293. DOI: 10.1007/s00266-006-0221-6.
99. F. Louis, Y. Sowa, S. Irie, S. Kitano, O. Mazda and M. Matsusaki, *Adv Healtcare Mater,* 2020, **11**, 2201440. DOI: 10.1002/adhm.202201440.
100. M. A. Abdul Sisak, F. Louis and M. Matsusaki, Polym J, 2020, **52**, 871-881. DOI: https://doi.org/10.1038/s41428-020-0331-z.
101. Y. C. Chiu, M. H. Cheng, S. Uriel and E. M. Brey, *J Tissue Viability*, 2011, **20**, 37–48. DOI: 10.1016/j.jtv.2009.11.005.
102. J. Han, J. E. Lee, J. Jin, J. S. Lim, N. Oh, K. Kim, S. I. Chang, M. Shibuya, H. Kim and G. Y. Koh, *Development*, 2011, **138**, 5027–5037. DOI: 10.1242/dev.067686.
103. K. J. Cronin, A. Messina, K. R. Knight, J. J. Cooper-White, G. W. Stevens, A. J. Penington and W. A. Morrison, *Plast Reconstr Surg*, 2004, **113**, 260-269. DOI: 10.1097/01.PRS.0000095942.71618.9D.
104. K. M. Abberton, S. K. Bortolotto, A. A. Woods, M. Findlay, W. A. Morrison, E. W. Thompson and A. Messina, *Cells Tissues Organs*, 2008, **188**, 347-358. DOI: 10.1159/000121575.
105. R. Yao, R. Zhang, J. Luan and F. Lin, *Biofabrication*, 2012, **4**, 025007. DOI: 10.1088/1758-5082/4/2/025007.
106. W. S. Kim, D. J. Mooney, P. R. Arany, K. Lee, N. Huebsch and J. Kim, *Tissue Eng Part A*, 2012, **18**, 737–743. DOI: 10.1089/ten.tea.2011.0250.
107. N. Davidenko, J. J. Campbell, E. S. Thian, C. J. Watson and R. E. Cameron, *Acta Biomater*, 2010, **6**, 3957–3968. DOI: 10.1016/j.actbio.2010.05.005.
108. K. H. Chang, H. T. Liao and J. P. Chen, *Acta Biomater*, 2013, **9**, 9012–9026. DOI: 10.1016/j.actbio.2013.06.046.
109. F. Louis, P. Pannetier, Z. Souguir, D. le Cerf, P. Valet, J. P. Vannier, G. Vidal and E. Demange, *Biotechnol Bioeng*, 2017, **114**, 1813–1824. DOI: 10.1002/bit.26306.

This journal is © The Royal Society of Chemistry 20xx

110. M. Halbleib, T. Skurk, C. de Luca, D. von Heimburg and H. Hauner, *Biomaterials*, 2003, **24**, 3125–3132. DOI: 10.1016/s0142-9612(03)00156-x.
111. L. Flynn, G. D. Prestwich, J. L. Semple and K. A. Woodhouse, *Biomaterials*, 2007, **28**, 3834–3842. DOI: 10.1016/j.biomaterials.2007.05.002.
112. D. Hanjaya-Putra, K. T. Wong, K. Hirotsu, S. Khetan, J. A. Burdick and S. Gerecht, *Biomaterials*, 2012, **33(26)**, 6126-6231. DOI: 10.1016/j.biomaterials.2012.05.027.
113. M. W. McCrary, D. Bousalis, S. Mobini, Y. H. Song and C. E. Schmidt, *Acta Biomater*, 2020, **111**, 1–19. DOI: https://doi.org/10.1016/j.actbio.2020.05.031.
114. J. S. Choi, B. S. Kim, J. Y. Kim, J. D. Kim, Y. C. Choi, H. J. Yang, K. Park, H. Y. Lee and Y. W. Cho, *J Biomed Mater Res A*, 2011, **97**, 292–299. DOI: 10.1002/jbm.a.33056.
115. D. A. Young, D. O. Ibrahim, D. Hu and K. L. Christman, *Acta Biomater*, 2011, **7**, 1040–1049. DOI: 10.1016/j.actbio.2010.09.035.
116. L. E. Flynn, *Biomaterials*, 2010, **31**, 4715–4724. DOI: 10.1016/j.biomaterials.2010.02.046.
117. M. K. DeBari, W. H. Ng, M. D. Griffin, L. E. Kokai, K. G. Marra, J. P. Rubin, X. Ren and R. D. Abbott, *Biomimetics*, 2021, **6**, 52. DOI:10.3390/biomimetics6030052.
118. L. S. Nair and C. T. Laurencin, *Prog Polym Sci*, 2007, **32**, 762–798. DOI: https://doi.org/10.1016/j.progpolymsci.2007.05.017.
119. S. W. Kang, S. W. Seo, C. Y. Choi and B. S. Kim, *Tissue Eng Part C Methods*, 2008, **14**, 25–34. DOI: 10.1089/tec.2007.0290.
120. J. A. Lee, B. M. Parrett, J. A. Conejero, J. Laser, J. Chen, A. J. Kogon, D. Nanda, R. T. Grant, A. S. Breitbart, C. Godek and J. E. Losee, *Ann Plast Surg*, 2003, **50**, 610–617. DOI: 10.1097/01.SAP.0000069069.23266.35.
121. D. Henn, K. Chen, K. Fischer, A. Rauh, J. A. Barrera, Y. J. Kim, R. A. Martin, M. Hannig, P. Niedoba, S. K. Reddy, H. Q. Mao, U. Kneser, G. C. Gurtner, J. M. Sacks and V. J. Schmidt, *Adv Wound Care (New Rochelle)*, 2020, **9**, 365–377. DOI: 10.1097/PRS.0000000000008872.
122. F. P. Brandl, A. K. Seitz, J. K. V. Teßmar, T. Blunk and A. M. Göpferich, *Biomaterials*, 2010, **31**, 3957–3966. DOI: 10.1016/j.biomaterials.2010.01.128.
123. A. Alhadlaq, M. Tang and J. J. Mao, *Tissue Eng*, 2005, **11**, 556–566. DOI: 10.1089/ten.2005.11.556.
124. X. Kang, Y. Xie and D. A. Kniss, *Tissue Eng*, 2005, **11**, 458–468. DOI: 10.1089/ten.2005.11.458.
125. E. Göktürk and H. Erdal, *SAÜ Fen Bilimleri Enstitüsü Dergisi*, 2017, **21**, 1237–1244. DOI: 10.16984/saufenbilder.283156.
126. C. Fischbach, T. Spruß, B. Weiser, M. Neubauer, C. Becker, M. Hacker, A. Göpferich and T. Blunk, *Exp Cell Res*, 2004, **300**, 54–64. DOI: 10.1016/j.yexcr.2004.05.036.
127. B. Weiser, L. Prantl, T. E. O. Schubert, J. Zellner, C. Fischbach-Teschl, T. Spruss, A. K. Seitz, J. Tessmar, A. Goepferich and T. Blunk, *Tissue Eng Part A*, 2008, **14**, 275–284. DOI: 10.1089/tea.2007.0130.
128. S. D. Lin, K. H. Wang and A. P. Kao, *Tissue Eng Part A*, 2008, **14**, 571–581. DOI: 10.1089/tea.2007.0192.
129. O. S. Manoukian, N. Sardashti, T. Stedman, K. Gailiunas, A. Ojha, A. Penalosa, C. Mancuso, M. Hobert and S. G. Kumbar, Encyclopedia of Biomedical Engineering, 2019, Elsevier: Oxford, 462-482.
130. R. M. Shanti, S. Janjanin, W. J. Li, L. J. Nesti, M. B. Mueller, M. B. Tzeng and R. S. Tuan, *Ann Plast Surg*, 2008, **61**, 566–571. DOI: 10.1097/SAP.0b013e31816d9579.
131. Y. Kambe, S. Ogino, H. Yamanaka, N. Morimoto and T. Yamaoka, *Biomed Mater Eng*, 2020, **31**, 203–210. DOI: 10.3233/BME-201103.
132. S. Liu, S. Qin, M. He, D. Zhou, Q. Qin and H. Wang, *Compos B Eng*, 2020, **199**, 108238. DOI: https://doi.org/10.1016/j.compositesb.2020.108238.
133. W. L. Haisler, D. M. Timm, J. A. Gage, H. Tseng, T. C. Killian and G. R. Souza, *Nat Protoc*, 2013, **8**, 1940–1949. DOI: 10.1038/nprot.2013.125.
134. R. Foty, *J Vis Exp*, 2011, **51**, e2720. DOI: 10.3791/2720.
135. J. Carlsson and J. M. Yuhas, *Recent Results Cancer Res*, 1984, **95**, 1–23. DOI: 10.1007/978-3-642-82340-4_1.
136. O. Sarigil, M. Anil-Inevi, B. Firatligil-Yildirir, Y. C. Unal, O. Yalcin-Ozuysal, G. Mese, H. C. Tekin and E. Ozcivici, *Biotechnol Bioeng*, 2020, **118**, 1127-1140. DOI: 10.1002/bit.27631.
137. B. Vu, G. R. Souza and J. Dengjel, *Matrix Biol Plus*, 2021, **11**, 100066. DOI: 10.1016/j.mbplus.2021.100066.
138. A. C. Daquinag, G. R. Souza and M. G. Kolonin, *Tissue Eng Part C Methods*, 2013, **19**, 336–344. DOI: 10.1089/ten.TEC.2012.0198.
139. S. Muller, I. Ader, J. Creff, H. Leménager, P. Achard, L. Casteilla, L. Sensebé, A. Carrière and F. Deschaseaux, *Sci Rep*, 2019, **9**, 1–10. DOI: https://doi.org/10.1038/s41598-019-43624-6.
140. H. Sugihara, N. Yonemitsu, S. Toda, S. Miyabara, S. Funatsumaru and T. Matsumoto, *J Lipid Res*, 1988, **29**, 691–697. DOI: https://doi.org/10.1016/S0022-2275(20)38514-X.
141. R. D. Hume, L. Berry, S. Reichelt, M. D'Angelo, J. Gomm, R. E. Cameron and C. J. Watson, *Tissue Eng Part A*, 2018, **24**, 1309–1319. DOI: 10.1089/ten.TEA.2017.0509.
142. F. Louis, S. Kitano, J. F. Mano and M. Matsusaki, *Acta Biomater*, 2019, **84**, 194–207. DOI: 10.1016/j.actbio.2018.11.048.
143. F. Louis, M. Piantino, H. Liu, D.-H. Kang, Y. Sowa, S. Kitano and M. Matsusaki, *Cyborg and Bionic Systems*, 2021, **2021**, 1–15. DOI: 10.34133/2021/1412542.
144. L. Hong, I. Peptan, P. Clark and J. J. Mao, *Ann Biomed Eng*, 2005, **33**, 511–517. DOI: 10.1007/s10439-005-2510-7.
145. L. Hong, I. A. Peptan, A. Colpan and J. L. Daw, *Cells Tissues Organs*, 2006, **183**, 133–140. DOI: 10.1159/000095987.

146. N. C. Negrini, N. Celikkin, P. Tarsini, S. Farè and W. Święszkowski, *Biofabrication*, 2020, **12**, 025001. DOI: 10.1088/1758-5090/ab56f9.
147. L. Tytgat, M. R. Kollert, L. van Damme, H. Thienpont, H. Ottevaere, G. N. Duda, S. Geissler, P. Dubruel, S. van Vlierberghe and T. H. Qazi, *Macromol Biosci*, 2020, **20**, 1–6. DOI: 10.1002/mabi.201900364.
148. B. Huber, K. Borchers, G. E. M. Tovar and P. J. Kluger, *J Biomater Appl*, 2016, **30**, 699–710. DOI: 10.1177/0885328215587450.
149. J. Colle, P. Blondeel, A. de Bruyne, S. Bochar, L. Tytgat, C. Vercruysse, S. van Vlierberghe, P. Dubruel and H. Declercq, *J Mater Sci Mater Med*, 2020, **31**, DOI:10.1007/s10856-020-06374-w.
150. Y. Kimura, T. Inamoto and Y. Tabata, *J Biomater Sci Polym Ed*, 2010, **21**, 463–476. DOI: 10.1163/156856209X424396.
151. J. R. Mauney, T. Nguyen, K. Gillen, C. Kirker-Head, J. M. Gimble and D. L. Kaplan, *Biomaterials*, 2007, **28**, 5280–5290. DOI: 10.1016/j.biomaterials.2007.08.017.
152. R. D. Abbott, R. Y. Wang, M. R. Reagan, Y. Chen, F. E. Borowsky, A. Zieba, K. G. Marra, J. P. Rubin, I. M. Ghobrial and D. L. Kaplan, *Adv Healthc Mater*, 2016, **5**, 1667–1677. DOI: 10.1002/adhm.201600211.
153. D. Henn, K. S. Fischer, K. Chen, A. H. Greco, R. A. Martin, D. Sivaraj, A. A. Trotsyuk, H. Q. Mao, S. K. Reddy, U. Kneser, G. C. Gurtner, V. J. Schmidt and J. M. Sacks, *Plast Reconstr Surg*, 2022, **149**, 433E-444E. DOI: 10.1097/PRS.0000000000008872
154. N. Contessi Negrini, N. Toffoletto, S. Farè and L. Altomare, *Front Bioeng Biotechnol*, 2020, **8**, 1–15. DOI: 10.3389/fbioe.2020.00723.
155. C. Fischbach, J. Seufert, H. Staiger, M. Hacker, M. Neubauer, A. Göpferich and T. Blunk, *Tissue Eng*, 2004, **10**, 215–229. DOI: 10.1089/107632704322791862.
156. Y.S. Choi, S. N. Park and H. Suh, *Biomaterials*, 2005, **26**, 5855–5863. DOI: 10.1016/j.biomaterials.2005.02.022.
157. M. Neubauer, M. Hacker, P. Bauer-Kreisel, B. Weiser, C. Fischbach, M. B. Schulz, A. Goepferich and T. Blunk, *Tissue Eng*, 2005, **11**, 1840–1851. DOI: 10.1089/ten.2005.11.1840.
158. Y. S. Choi, S. M. Cha, Y. Y. Lee, S. W. Kwon, C. J. Park and M. J. Kim, *Biochem Biophys Res Commun*, 2006, **345**, 631–637. DOI: 10.1016/j.bbrc.2006.04.128.
159. L. W. Dunne, Z. Huang, W. Meng, X. Fan, N. Zhang, Q. Zhang and Z. An, *Biomaterials*, 2014, **35**, 4940–4949. DOI: 10.1016/j.biomaterials.2014.03.003.
160. A. J. Klingelhutz, F. A. Gourronc, A. Chaly, D. A. Wadkins, A. J. Burand, K. R. Markan, S. O. Idiga, M. Wu, M. J. Potthoff and J. A. Ankrum, *Sci Rep*, 2018, **8**, 1–12. DOI: 10.1038/s41598-017-19024-z.
161. P. Loskill, T. Sezhian, K. M. Tharp, F. T. Lee-Montiel, S. Jeeawoody, W. M. Reese, P. J. H. Zushin, A. Stahl and K. E. Healy, *Lab Chip*, 2017, **17**, 1645–1654. DOI: 10.1039/c6lc01590e.
162. J. Rogal, C. Binder, E. Kromidas, C. Probst, S. Schneider, K. Schenke-Layland and P. Loskill, *Sci Rep*, 2020, **10,** 1-12. DOI: 10.1038/s41598-020-63710-4.
163. C. S. Murphy, L. Liaw and M. R. Reagan, *BMC Biomed Eng*, 2019, **1**, 1–19. DOI: 10.1186/s42490-019-0027-7.
164. G. Y. Kim, S. J. Yeom, S. C. Jang, C. S. Lee, C. Roh and H. H. Jeong, *Biomolecules*, 2018, **8**, 37. DOI: 10.3390/biom8020037.
165. F. Yang, A. Carmona, K. Stojkova, E. I. Garcia Huitron, A. Goddi, A. Bhushan, R. N. Cohen and E. M. Brey, *Lab Chip*, 2020, **21**, 435-446. DOI:10.1039/d0lc00981d.
166. P. Loskill, S. G. Marcus, A. Mathur, W. M. Reese and K. E. Healy, *PLoS One*, 2015, **10**, 1–13. DOI: 10.1371/journal.pone.0139587.
167. M. McCarthy, T. Brown, A. Alarcon, C. Williams, X. Wu, R. D. Abbott, J. Gimble and T. Frazier, *Tissue Eng Part B Rev*, 2020, **26**, 586-595. DOI: 10.1089/ten.TEB.2019.0261.
168. V. D. Dahik, E. Frisdal and W. le Goff, *Int J Mol Sci*, 2020, **21**, 1–30. DOI:10.3390/ijms21155505.
169. Y. T. Wondmkun, *Diabetes Metab Syndr Obes*, 2020, **12**, 3611-3616. DOI: 10.2147/DMSO.S275898.
170. T. Khan, E. S. Muise, P. Iyengar, Z. v. Wang, M. Chandalia, N. Abate, B. B. Zhang, P. Bonaldo, S. Chua and P. E. Scherer, *Mol Cell Biol*, 2009, **29**, 1575–1591. DOI: 10.1128/MCB.01300-08.
171. O. Huttala, J. R. Sarkanen, M. Mannerström, T. Toimela, T. Heinonen and T. Ylikomi, *Cytotechnology*, 2020, **72**, 665–683. DOI: 10.1007/s10616-020-00407-6.
172. S. Cinti, G. Mitchell, G. Barbatelli, I. Murano, E. Ceresi, E. Faloia, S. Wang, M. Fortier, A. S. Greenberg and M. S. Obin, *J Lipid Res*, 2005, **46**, 2347–2355. DOI: 10.1194/jlr.M500294-JLR200.
173. M. Keuper, *Endocr Connect*, 2019, **8**, 105–121. DOI: 10.1530/EC-19-0016.
174. J. H. Choi, J. M. Gimble, G. Vunjak-Novakovic and D. L. Kaplan, *Tissue Eng Part C Methods*, 2010, **16**, 1157-1165. DOI: 10.1089/ten.tec.2009.0760.
175. A. Ioannidou, S. Alatar, R. Schipper, F. Baganha, M. Åhlander, A. Hornell, R. M. Fisher, C. E. Hagberg, K. Barrett and M. Chondronikola, *J Physiol*, 2021, **0**, 1–15. DOI: 10.1113/JP281445.
176. R. K. C. Loh, B. A. Kingwell and A. L. Carey, *Obesity Reviews*, 2017, **18**, 1227-1242. DOI:10.1111/obr.12584.
177. V. S. LeBleu, B. MacDonald and R. Kalluri, *Exp Biol Med*, 2007, **232**, 1121–1129. DOI: 10.3181/0703-MR-72.
178. A. S. Charonis, E. C. Tsilibary, T. Saku and H. Furthmayr, *J Cell Biol,* 1986, **103**, 1689-1697. DOI: 10.1083/jcb.103.5.1689.
179. M. K. Vaicik, M. Morse, A. Blagajcevic, J. Rios, J. C. Larson, F. Yang, R. N. Cohen, G. Papavasiliou and E. M. Brey, *J Mater Chem B*, 2015, **3**, 7903–7911. DOI: 10.1039/C5TB00952A.

This journal is © The Royal Society of Chemistry 20xx

180. M. di Somma, W. Schaafsma, E. Grillo, M. Vliora, E. Dakou, M. Corsini, C. Ravelli, R. Ronca, P. Sakellariou, J. Vanparijs, B. Castro and S. Mitola, *Cells*, 2019, **8**, 1457. DOI: 10.3390/cells8111457.
181. A. Weinzierl, Y. Harder, D. Schmauss, E. Ampofo, M. D. Menger and M. W. Laschke, *Biomedicines*, 2022, **10**, 23. DOI: 10.3390/biomedicines10010023.
182. M. Bagchi, L. A. Kim, J. Boucher, T. E. Walshe, C. R. Kahn and P. A. D'amore, *The FASEB Journal,* 2013*,* **28**, 3257-3271. DOI: 10.1096/fj.12-221812.
183. M. Kuss, J. Kim, D. Qi, S. Wu, Y. Lei, S. Chung and B. Duan, *Acta Biomater*, 2018, **71**, 486–495. DOI: 10.1016/j.actbio.2018.03.021
184. A. L. Hafner, J. Contet, C. Ravaud, X. Yao, P. Villageois, K. Suknuntha, K. Annab, P. Peraldi, B. Binetruy, I. I. Slukvin, A. Ladoux and C. Dani, *Sci Rep*, 2016, **6**, 1-9. DOI: 10.1038/srep32490.
185. F. S. Frueh, T. Später, C. Scheuer, M. D. Menger and M. W. Laschke, *J Vis Exp*, 2017, **122**, e55721. DOI: 10.3791/55721.
186. F. M. Acosta, K. Stojkova, J. Zhang, E. I. Garcia Huitron, J. X. Jiang, C. R. Rathbone and E. M. Brey, *J Tissue Eng*, 2022, **13**, p.20417314221109337. DOI: 10.1177/20417314221109337.
187. M. A. Gonzalez Porras, K. Stojkova, F. M. Acosta, C. R. Rathbone and E. M. Brey, *Front Bioeng Biotechnol*, 2022, **10**. DOI: 10.3389/fbioe.2022.906395.
188. H. Sung, J. Ferlay, R. L. Siegel, M. Laversanne, I. Soerjomataram, A. Jemal and F. Bray, *CA Cancer J Clin*, 2021, **71**, 209–249. DOI: 10.3322/caac.21660.
189. M. Abdul-Al, A. Zaernia and F. Sefat, *J Tissue Eng Regen Med*, 2020, **14**, 1549–1569. DOI: 10.1002/term.3121
190. T. R. Kosowski, G. Rigotti and R. K. Khouri, *Clin Plast Surg*, 2015, **42**, 325–337. DOI: 10.1016/j.cps.2015.03.001.
191. M. P. Chhaya, E. R. Balmayor, D. W. Hutmacher and J. T. Schantz, *Sci Rep*, 2016, **6**, 1-12. DOI: 10.1038/srep28030.
192. L. Benmeridja, L. de Moor, E. de Maere, F. Vanlauwe, M. Ryx, L. Tytgat, C. Vercruysse, P. Dubruel, S. van Vlierberghe, P. Blondeel and H. Declercq, *J Tissue Eng Regen Med*, 2020, **14**, 840-854. DOI: 10.1002/term.3051.
193. S. Hou, X. Wang, S. Park, X. Jin and P. X. Ma, *Adv Healthc Mater*, 2015, **4**, 1491-1495. DOI: 10.1002/adhm.201500093.
194. S. W. Cho, S. S. Kim, J. W. Rhie, H. M. Cho, C. Y. Choi and B. S. Kim, *Biomaterials*, 2005, **26**, 3577–3585.
195. DOI: 10.1016/j.biomaterials.2004.09.013.
196. F. Pati, J. Gantelius and H. A. Svahn, *Angew Chem Int Ed*, 2016, **55**, 4650-4665. DOI: 10.1002/anie.201505062.
197. K. Säljö, L. S. Orrhult, P. Apelgren, K. Markstedt, L. Kölby and P. Gatenholm, *Bioprinting*, 2020, **17**, e00065. DOI: 10.1016/j.bprint.2019.e00065.